Theoretical investigation of magnetically induced currents in closed-shell molecules

Dissertation for the degree of Doctor Philosophiae

Jonas Jusélius

University of Helsinki
Department of Chemistry
Laboratory for Instruction in Swedish
P.O. Box 55 (A.I. Virtasen Aukio 1)
FIN-00014 University of Helsinki, Finland

To be presented, with the assent of the Faculty of Science, University of Helsinki, for public discussion in Auditorium A129, Department of Chemistry (A.I. Virtasen Aukio 1, Helsinki), December the 20th, 2004, at noon.

Helsinki 2004

Supervised by

Dr. Dage Sundholm
Department of Chemistry
University of Helsinki

Reviewed by

Prof. Kenneth Ruud
Department of Chemistry
University of Tromsø

Dr. Juha Vaara
Department of Chemistry
University of Helsinki

Abstract

The work presented in this thesis is concerned with the theory and development of methods for *ab initio* calculation of magnetically induced current densities in closed-shell molecules. Two new methods are presented. The underlying theory of both methods is closely related to the theory of nuclear magnetic shielding (NMR) calculations. The Aromatic Ring-Current Shieldings (ARCS) method can be viewed as an experimental procedure in a theoretical framework. In the ARCS method, the strength of the magnetically induced ring current in aromatic molecules is extracted from the long-range part of the calculated NMR shielding function through a fitting procedure.

In the Gauge-Including Magnetically Induced Currents (GIMIC) method, the magnetically induced current density in molecules is calculated explicitly. In order to overcome problems with the dependence on the magnetic gauge origin, Gauge-Including Atomic Orbitals (GIAOs) are employed. The advantage of the GIMIC method is high accuracy, and the applicability to mean-field, density-functional and electron-correlated levels of theory. The GIMIC method is fast and can be applied to large closed-shell molecules of nano-technological importance. The method can also reveal the detailed structure of the current density in molecules. Using quadrature, the GIMIC method can be used to obtain the strength of induced currents in aromatic molecules.

The ARCS and GIMIC methods have been applied to a variety of different molecular systems, both to test their applicability and accuracy, and in an attempt to understand and classify molecular aromaticity.

List of publications

List of publications included in the thesis

I. J. Jusélius and D. Sundholm, *Ab initio determination of the induced ring current in aromatic molecules*, Phys. Chem. Chem. Phys., **1**, 3429 (1999).

II. J. Jusélius and D. Sundholm, *The aromatic pathways of porphins, chlorins and bacteriochlorins*, Phys. Chem. Chem. Phys., **2**, 2145 (2000).

III. J. Jusélius and D. Sundholm, *The aromatic character of magnesium porphyrins*, J. Org. Chem., **65**, 5233 (2000).

IV. J. Jusélius and D. Sundholm, *The aromaticity and antiaromaticity of dehydroannulenes*, Phys. Chem. Chem. Phys., **3**, 2433 (2001).

V. J. Jusélius, M. Straka, and D. Sundholm, *Magnetic Shielding Calculations on Al_4^{2-} and Analogues*, J. Phys. Chem. A, **105**, 9939 (2001).

VI. J. Jusélius, M. Patzschke, and D. Sundholm, *Calculation of Ring-Current Susceptibilites for Potentially Homoaromatic Hydrocarbons*, J. Mol. Struct. (Theochem), **633**, 123 (2003).

VII. J. Jusélius, D. Sundholm, and J. Gauss, *Calculation of Current Densities using Gauge-Including Atomic Orbitals*, J. Chem. Phys., **121**, 3952 (2004).

List of other publications

I. R. J. F. Berger, M. A. Schmidt, J. Jusélius, D. Sundholm, P. Sirsch, and H. Schmidbaur, *Tetraberyllium-η^4-oxo-hexa(arylcarboxylates)*, Z. Naturforsch. b, **56**, 979 (2001).

II. E. M. S. Maçôas, L. Khriachtchev, M. Petterson, J. Jusélius, R. Fausto, and M. Räsänen, *Reactive vibrational excitation spectroscopy of formic acid in solid argon: Quantum yield for infrared induced trans→cis isomerization and solid state effects on the vibrational spectrum*, J. Chem. Phys., **119**, 11765 (2004).

III. M. Johansson and J. Jusélius, *Arsole aromaticity revisited*, Lett. Org. Chem. (2004), accepted.

IV. L. Khriachtchev, J. Jusélius, A. Lignell, M. Räsänen, and E. Savchenko, *Infrared absorption spectrum of matrix-isolated noble-gas hydride molecules: Fingerprints of specific interactions and hindered rotation*, J. Chem. Phys. (2004), accepted.

V. D. Sundholm, M. Johansson, and J. Jusélius, *Sphere currents of Buckminsterfullerene*, Angew. Chem. Int. Ed. (2004), accepted.

VI. Y. C. Lin, J. Jusélius, D. Sundholm, and J. Gauss, *Calculation of Current Densities in Al_4^{2-}*, Angew. Chem. Int. Ed. (2004), to be published.

Acknowledgments

I would like to express my deepest gratitude to my supervisor Dage Sundholm, who is an excellent scientist, a top-notch supervisor and a good friend. In his good-humored way, he always seems to find time to listen and help. He also knows when to come and "kick in my door" and give me a push, without interfering more than needed. I thank Pekka Pyykkö for hiring me to the group already in my second year at the university. I consider Pekka my second supervisor, since he has spent numerous hours explaining and teaching me both quantum mechanics and chemistry. Pekka's enormous knowledge in physics, quantum mechanics and chemistry has been an invaluable asset during my studies. I also jointly thank Pekka and Dage for sending me to many research schools and conferences over the years.

I owe a lot of gratitude to the past and present members of the Laboratory of Instruction in Swedish: Mikael Johansson, Henrik Konschin, Olli Lehtonen, Ying-Chan Lin, Bjarne Lindström, Michael Patzschke, Stefan Taubert, Bertel Westermark, Pekka Manninen, Michaela Ekholm, Carola Olkkonen, Nino Runeberg, Toomas Tamm, Henrik Tylli and Juha Vaara. I thank you for what you have taught me, for proof-reading manuscripts and all the discussions in the coffee room, ranging from chemistry to politics. One person who deserves an extra big thank-you is the sunshine of the laboratory, Susanne Lundberg, who somehow always manages to be in a cheerful mood and never fails to be helpful.

I especially want to thank Jürgen Gauss for inviting me to Mainz, and for his great hospitality during my stays. I had a very good time in Mainz, both scientifically and socially, not least thanks to the Mainz group at the time: Alexander Auer, Michael Harding, Miriam Heckert, Oliver Heun, Uli Häberle, Dan Jonsson, Mihály Kállay, Michael Lenhart and Thorsten Metzroth.

I also want to thank my co-authors for many fruitful collaborations: Raphael Berger, Rui Fausto, Jürgen Gauss, Mikael Johansson, Leonid Khriachtchev, Antti Lignell, Ying-Chan Lin, Ermelinda Maçôas, Michael Patzschke, Mika Petterson, Markku Räsänen, Elena Savchenko, Michal Straka and Dage Sunholm. I thank Magnus Ehrnrooths stiftelse, Waldemar von Frenkells stiftelse, the LASKEMO graduate school, the Academy of Finland and the University of Helsinki for their generous support.

Last, but not least, I want to thank my family and friends. I thank my brothers, Mikael and Joakim Jusélius for just being there. My mother Katarina Jusélius, and Søren Johansen I thank for their enourmous support, and for the beautiful summers at Trollön. I also thank my father Jussi Jusélius, and Tuula Jusélius for being supportive. My grandmother, Maija Jusélius deserves a huge hug for being there for me, and for cooking wonderful dinners every Sunday. I also thank my godmother Kaisa Lillqvist, and my Danish "brothers" for being so nice. I want to thank Tommy Vänskä for being such a good friend, for the rock climbing trips around Europe, for the countless hours in the pool hall, and for the afternoons on Trollön, sitting in the sun and contemplating quantum mechanics.

Finally, I want to express my greatest gratitude to my love, Mia Tenhunen, for putting up with me, and always supporting me. You have taught me so many things that cannot be aquired by reading books. I thank you for your patience and understanding, for being a worthy opponent, but most of all, for just being you. I also silently thank the rest of my good friends, you know how you are, but you are too many to fit on this page.

Jonas Jusélius

Helsinki, 10th June 2005

Contents

List of abbreviations

AO	Atomic Orbital
ARCS	Aromatic Ring-Current Shielding
CC	Coupled-Cluster
CCSD	Coupled-Cluster with Single and Double excitations
CHF	Coupled Hartree–Fock
CI	Configuration Interaction
CSGT	Continuous Set of Gauge Transformations
CTOCD	Continuous Transformation of Origin of the Current Density
CPHF	Coupled Perturbed Hartree–Fock
DFT	Density-Functional Theory
GIMIC	Gauge-Including Magnetically Induced Current
GIAO	Gauge-Including Atomic Orbital
GTO	Gaussian Type Orbital
HF	Hartree–Fock
LCAO	Linear Combination of Atomic Orbitals
MBPT	Many-Body Perturbation Theory
MP2	Møller–Plesset perturbation theory to the second order
MO	Molecular Orbital
NICS	Nucleus-Independent Chemical Shift
NMR	Nuclear Magnetic Resonance
PARCS	Planar Aromatic Ring-Current Shielding
SCF	Self-Consistent Field

Chapter 1

Introduction

Aromaticity is an important concept in chemistry. Although widely used, the aromaticity concept is not uniquely defined. High stability, reduced bond length alternation, low reactivity and increased response to magnetic fields are typical characteristics for aromatic molecules. One of the motivations for starting the work presented in this thesis was to try to understand the chemical concept of aromaticity from a theoretical point of view.

For a long time, aromaticity was considered to be a property of only cyclic, planar organic molecules having $4n+2$ π-electrons. However, the concept of aromaticity has later been extended to include also inorganic and non-planar, spherical and even linear molecules! The idea that only the π-electrons contribute to aromaticity has been revised to include σ-electrons. Aromaticity has previously been defined on the basis of energetics, as well as geometric and magnetic criteria, such as nuclear magnetic shielding tensors and magnetic susceptibilities [14, 15, 16, 17, 18, 19, 20, 21, 22, 23, 24, 25, 26, 27, 28, 29]. The degree of aromaticity is even more difficult to deduce from energetic and structural data than from magnetic criteria such as elevated magnetic susceptibility, susceptibility anisotropies, and Nucleus-Independent Chemical Shift (NICS) values [24]. With this in mind it might seem futile to try to come up with a single theoretical model which would be able to quantify aromaticity.

While aromaticity, like beauty, may be in the eye of the beholder, the magnetically induced currents in a molecule are unequivocally defined. In the pursuit to understand and quantify aromaticity a very pragmatic view is hence adopted here. The key molecular property for a molecule to be aromatic is the ability to sustain a *net* electrical current when subjected to a magnetic field. A ring current does itself not guarantee aromaticity, but failure to sustain a ring current guarantees that the molecule is not aromatic. Throughout this thesis the word aromaticity is used as a synonym for "ability to sustain a ring current", regardless of any other aromatic properties.

The calculation of time-independent ring currents of closed-shell molecules, and the strength of the currents are the main topic of this thesis. Whether the strengths of these currents can be used to classify aromatic strength can be debated. In order to lay the foundation for understanding the work presented in this thesis, I will review the most important aspects of the underlying theoretical framework. Chap. 2 gives a short review of the Schrödinger equation and the most common approximations and methods for calculating the molecular ground-state energy. In Chap. 3 general methods for obtaining molecular ground-state properties are discussed, with focus on derivative theory. The theory of magnetic interactions, and in particular interactions between electrons and an external magnetic field, are considered in Chap. 4. Chap. 4 also touches the subject of calculating nuclear magnetic shielding parameters, and the problem of gauge invariance. Ring currents and aromaticity are discussed in some detail in Chap. 5, with examples of various kinds of aromaticity. Chap. 5 also presents the theory underlying our first quantitative method for estimating the strength of the ring current, the Aromatic Ring-Current Shieldings (ARCS) method [1]. In Chap. 6 *ab initio* ring-current models are presented, with an in-depth discussion of the new Gauge-Including Magnetically Induced Currents (GIMIC) method [7]. Chap. 7 provides an

summary of the original scientific papers included in the appendices.

Chapter 2

The molecular energy

In this chapter some of the standard methods and approximations of quantum chemistry are reviewed. Only the theory of time-independent, closed-shell molecules in a non-relativistic framework will be considered.

The starting point for most of quantum chemistry is the time-independent Schrödinger equation which can be compactly written $\hat{H}\Psi = E\Psi$, where $\hat{H}$ is the Hamiltonian and Ψ is the wave function. In atomic units* the molecular Hamiltonian in its simplest form is given by

$$\hat{H} = -\frac{1}{2}\sum_i^N \nabla_i^2 + \sum_{i>j}^N \frac{1}{r_{ij}} - \sum_A^K \sum_i^N \frac{Z_A}{r_{Ai}} - \sum_A^K \frac{1}{2M_A}\nabla_A^2 + \sum_{A>B}^K \frac{Z_A Z_B}{R_{AB}}, \tag{2.1}$$

where N is the number of electrons, K the number of nuclei, M_K the nuclear mass and Z_A the nuclear charge. The operator r_{ij} is the inter-electronic distance between electrons i and j. Using the Born–Oppenheimer approximation [30] the nuclear degrees of freedom can be separated from the electronic degrees of freedom, and the (time-independent) wave function then depends only parametrically on the nuclear coordinates. The wave function is then dependent on $4N$ variables, including the electron spin. Already for moderately complicated molecules, containing hundreds or thousands of electrons, this function quickly becomes extremely complicated.

The electronic wave function must be square integrable and normalized to be consistent with the Born probability interpretation [31]

$$1 = \int d\mathbf{x}_1 \dots d\mathbf{x}_N \Psi(\mathbf{x}_1 \dots \mathbf{x}_N)^* \Psi(\mathbf{x}_1 \dots \mathbf{x}_N), \tag{2.2}$$

where Ψ^* denotes the complex conjugate and $\mathbf{x} = (r_1, r_2, r_3, \sigma)$, where $\sigma \in \{\alpha, \beta\}$ is the electron spin coordinate. In closed-shell molecules the spin can be be integrated out, leaving three spatial degrees of freedom per electron.

In accordance with the above condition the electron density of the system is

$$\rho(\mathbf{r}) = N \int d\mathbf{r}_2 \dots d\mathbf{r}_N \Psi(\mathbf{r}, \mathbf{r}_2, \dots \mathbf{r}_N)^* \Psi(\mathbf{r}, \mathbf{r}_2, \dots \mathbf{r}_N). \tag{2.3}$$

To deal with this formidable function, one usually expands it in a basis of $3N$-dimensional functions. The basis functions are formed by anti-symmetrizing direct products of N one-particle functions with respect to the particle indices. These functions can conveniently be written as Slater determinants, $\Phi = \det|\phi_p(\mathbf{r}_1) \dots \phi_q(\mathbf{r}_N)|$. The one-particle functions are usually taken as linear combinations of atom-centered functions

$$\phi_a(\mathbf{r}) = \sum_\mu^{N_{AO}} C_{\mu a}\chi_\mu(\mathbf{r}), \tag{2.4}$$

---

*In atomic units $e = \hbar = m_e = 4\pi\epsilon_0 = 1$.

optimized to loosely resemble atomic orbitals. This expansion thus views the molecule as a linear combination of atoms, and the expanded functions are commonly referred to as molecular orbitals (MOs). This is somewhat misleading, and the procedure is best viewed as a practical way of generating a compact basis set expansion.

The atom-centered functions, referred to as atomic orbitals (AOs), are usually constructed from fixed linear combinations of Gaussian Type Orbitals (GTOs)

$$\chi_\mu(\mathbf{r}) = \sum_\xi w_{\xi\mu} r_x^{l_x} r_y^{l_y} r_z^{l_z} e^{-\alpha_{\xi\mu}\mathbf{r}^2}, \qquad (2.5)$$

where $\alpha_{\xi\mu}$ are orbital exponents, $w_{\xi\mu}$ are contraction coefficients and the prefactor exponents $\{l_{\{x,y,z\}} \in Z_+\}$ are related to the orbital angular momentum quantum number. The coordinates are given relative to the origin $\mathbf{R}_\mu$ of the basis function, $r_\beta = r'_\beta - R_{\mu\beta}$. The primary reason for using Gaussians is due to their locality and appealing properties for integral calculations.

In a similar manner, a function of two variables can be expanded by considering the expansion coefficients in Eq. 2.4 as functions of the second variable. This function can again be expanded in the same basis

$$\Phi(\mathbf{r}_1, \mathbf{r}_2) = \sum_\mu C_\mu(\mathbf{r}_2)\chi_\mu(\mathbf{r}_1) = \sum_{\mu\nu} C_{\mu\nu}\chi_\mu(\mathbf{r}_1)\chi_\nu(\mathbf{r}_2). \qquad (2.6)$$

Generalizing, the exact N-particle wave function can be written

$$\Psi = \sum_k c_k \sum_{n=1}^{N!} (-1)^{p_n} \mathcal{P}_n \prod_i^N \phi_i^{\{k\}}(\mathbf{r}_i) \qquad (2.7)$$

where $\{k\}$ denotes the k:th unique set of MOs from all possible sets. In order to ensure fermionic symmetry of the wave function, a permutation operator $\mathcal{P}_n$, has been included. $\mathcal{P}_n$ generates the n:th permutation of the electronic coordinates $\mathbf{r}_i$, and p_n is the number of transpositions needed to generate the permutation.

Henceforth, Slater determinants will be denoted $\Phi_s = |\phi_p \ldots \phi_t\rangle$, and integrals over Slater determinants will be denoted $\langle\Phi_p|\hat{O}|\Phi_q\rangle$, where an arbitrary operator has been included. The following convention will be used regarding indices: $i, j \ldots$ refer to occupied orbitals*, $a, b \ldots$ refer to unoccupied orbitals and $p, q \ldots$ are general indices. Greek letters will used for atomic orbital basis function indices.

A very elegant way of constructing a wave function of the proper symmetry, is through the formalism of second quantization. Second quantization revolves around a set of abstract operators acting on Slater determinants. An electron is created in a spin-orbital ϕ_p from the vacuum by the *creation operator*, $a_p^\dagger|\phi_q\phi_r\rangle = |\phi_p\phi_q\phi_r\rangle$. The conjugate operator is called an *annihilation operator*, $a_p|\phi_p\phi_q\phi_r\rangle = |\phi_q\phi_r\rangle$ $(p \neq q, r)$, which destroys the electron in a spin-orbital ϕ_p. In fermionic systems, acting with a creation operator on an occupied state gives zero, $a_p^\dagger|\phi_p\phi_q\rangle = 0$, and conversely for the annihilation operators $a_p|\phi_q\phi_r\rangle = 0$. Furthermore, the following anticommutation relations hold for the creation and annihilation operators

$$\left.\begin{array}{l} \{a_p^\dagger, a_q^\dagger\} = a_p^\dagger a_q^\dagger + a_q^\dagger a_p^\dagger = 0 \\ \{a_p, a_q\} = a_p a_q + a_q a_p = 0 \\ \{a_p, a_q^\dagger\} = a_p a_q^\dagger + a_q^\dagger a_p = \delta_{pq} \end{array}\right\} \Rightarrow \begin{array}{l} a_p^\dagger a_q^\dagger = -a_q^\dagger a_p^\dagger \\ a_p a_q = -a_q a_p \\ a_p a_q^\dagger = \delta_{pq} - a_q^\dagger a_p \end{array}. \qquad (2.8)$$

This definition of the operators ensures the proper antisymmetry of the wave function.

Using the formalism of second quantization, the electronic Hamiltonian can be written in terms of creation and annihilation operators

$$\hat{H} = \sum_{pq} h_{pq} a_p^\dagger a_q + \frac{1}{4} \sum_{pqrs} g_{pqrs} a_p^\dagger a_q^\dagger a_s a_r, \qquad (2.9)$$

---

*See Sec. 2.1.1 for a definition of occupied and unoccupied orbitals.

where h_{pq} and g_{pqrs} are given by the integrals

$$h_{pq} = \langle \phi_p(1)|\hat{h}|\phi_q(1)\rangle \quad \text{with} \quad \hat{h} = -\frac{1}{2}\nabla^2(1) - \sum_A^K \frac{Z_A}{r_{1A}} \tag{2.10}$$

$$g_{pqrs} = \langle \phi_p(1)\phi_q(2)|r_{12}^{-1}|\phi_r(1)\phi_s(2)\rangle - \langle \phi_p(1)\phi_q(2)|r_{12}^{-1}|\phi_s(1)\phi_r(2)\rangle = \langle pq||rs\rangle. \tag{2.11}$$

Applying the second-quantized Hamiltonian to a reference wave function, and using the anti-commutation relations in Eq. 2.8, the energy expression can be reduced to involve only specific integrals and orbital coefficients. The energy can then be written very compactly in matrix notation

$$E = \sum_{\mu\nu} h_{\mu\nu} D_{\mu\nu} + \frac{1}{2} \sum_{\mu\nu\sigma\rho} g_{\mu\sigma\nu\rho} d_{\mu\sigma\nu\rho}, \tag{2.12}$$

where the orbital coefficients are contained in the one- and two-body density matrices $D_{\mu\nu}$ and $d_{\mu\sigma\nu\rho}$. Similarly to Eq. 2.10 and Eq. 2.11, the AO representation of the one- and two-electron interaction integrals are

$$h_{\mu\nu} = \langle \chi_\mu|\hat{h}|\chi_\nu\rangle \quad \text{and} \quad g_{\mu\sigma\nu\rho} = \langle \chi_\mu\chi_\sigma||\chi_\nu\chi_\rho\rangle. \tag{2.13}$$

2.1 Computational methods

So far no approximations have been made, provided we expand the wave function in an infinite number of basis functions. In practice one is always forced to use a finite number of AOs, which truncates the MO expansion since the number of MOs is equal to the number of AOs. Truncation of the basis set naturally truncates the total wave-function expansion, but regardless of this, the expansion is completely intractable for anything but the simplest systems. We shall now look at some of the most common approximations for the wave function.

2.1.1 The mean-field approximation

The computationally least demanding *ab initio* wave-function based method for calculating the molecular energy is the Hartree–Fock (HF) approximation. In the HF approximation the wave-function expansion in Eq. 2.7 is truncated at the first term, *i.e.* the wave function is described by one Slater determinant. Since a Slater determinant is a direct product of one-particle functions, this implies a description where the electrons move independently of each other, in the mean potential of the other electrons and nuclei.

The energy of a one-determinant trial function is

$$E[\Phi] = \langle \Phi|\hat{H}|\Phi\rangle = \sum_i \langle \phi_i|\hat{h}|\phi_i\rangle + \frac{1}{2}\sum_{ij}\left(\langle \phi_i\phi_j|r_{12}^{-1}|\phi_i\phi_j\rangle - \langle \phi_i\phi_j|r_{12}^{-1}|\phi_j\phi_i\rangle\right)$$

$$= \sum_i \langle \phi_i|\hat{h}|\phi_i\rangle + \frac{1}{2}\sum_{ij}\langle \phi_i|(J_j - K_j)|\phi_i\rangle, \tag{2.14}$$

where J is the Coulomb operator, describing the interaction between two charge distributions, and K is the exchange operator, arising from the anti-symmetry of the wave function. Linear variation of the trial function, Φ, under the constraint that the one-particle functions remain orthonormal, $\langle \phi_p|\phi_q\rangle = \delta_{pq}$, yields the Hartree–Fock equations

$$f\phi_i = \epsilon_i\phi_i, \tag{2.15}$$

where the Fock operator is

$$f(1) = \hat{h}(1) + \sum_i (J_i(1) - K_i(1)) = h(1) + v^{HF}(1). \tag{2.16}$$

Solving the Hartree–Fock equations yields a set of eigenfunctions, the molecular orbitals, and the corresponding eigenvalues, the orbital energies. The molecular orbitals form a complete orthonormal set in the space spanned by the basis, and are obtained as the MO coefficients in Eq. 2.4. The variational principle [32] ensures that the energy of an approximate wave function is always higher than the true energy of the system. The equations must be solved iteratively, until self-consistency is reached, since the HF potential is a functional of its eigenfunctions.

It should be noted that the molecular orbitals are not unique, and the energy is invariant to unitary transformations of the molecular orbitals. One should be very careful in trying to ascribe any real physical meaning to the molecular orbitals. The N orbitals of lowest energy are referred to as occupied orbitals, and the complementary set as virtual or unoccupied orbitals. The single-determinant ground-state wave function, Ψ_0, is obtained from the direct product of the occupied orbitals.

The eigenvalue of the total Fock operator, $F = \sum_i f(i)$, acting on the ground-state wave function is

$$F|\Psi_0^{HF}\rangle = E_0|\Psi_0^{HF}\rangle, \tag{2.17}$$

where $E_0 = \sum_i^N \epsilon_i$. It is important to realize that this eigenvalue is not the ground-state energy, due to double counting of the electron-electron interactions. The true Hartree–Fock ground state energy is

$$E_{HF} = \sum_i^N \epsilon_i - \frac{1}{2}\sum_{ij}^N \langle\phi_i|(J_j - K_j)\phi_i\rangle, \tag{2.18}$$

which is not an eigenvalue of the Fock operator. The computational work needed to solve the Hartree-Fock equations scales formally as $O(\mathcal{N}^4)$ with respect to the system size, where $\mathcal{N}$ is related to the number of occupied and unoccupied orbitals.

The mean-field energy is not the exact energy of the system, but it is often a good approximation. The energy difference between the mean-field energy and the exact energy is due to electron correlation, *i.e.* the fact that electrons do *not* move independently of each other. Electron correlation lowers the energy by reducing the probability of electrons being in the vicinity of each other, thereby reducing the electron-electron repulsion. The correlation energy is defined as the difference between the Hartree–Fock energy and the (unknown), exact non-relativistic energy [33]

$$E_{corr} = E_{HF} - E_{exact}. \tag{2.19}$$

Determinants where one or more occupied orbitals have been substituted by virtual orbitals, symbolically $\Psi_0(i \to a, j \to b) = \Psi_{ij}^{ab}$, are called excited determinants. In principle it is easy to recover the correlation energy, in a given finite N-particle subspace generated by the one-particle orbitals, by diagonalizing the Hamiltonian in the basis of all unique excited determinants

$$\Psi = \Phi_0 + \sum_{ia} c_i^a \Phi_i^a + \sum_{ijab} c_{ij}^{ab} \Phi_{ij}^{ab} + \ldots + \sum_{ij\ldots n} \sum_{ab\ldots q} c_{ij\ldots n}^{ab\ldots q} \Phi_{ij\ldots n}^{ab\ldots q} \tag{2.20}$$

This approach, called Full Configuration Interaction (FCI), has one major practical drawback. The number of determinants in the N-particle basis grows approximately as $\binom{2K}{N}$, where K is the number of basis functions and N is the number of electrons. For a small system like benzene with 42 electrons in a small basis with 120 functions, the number of unique determinants is of the order 10^{47}. Diagonalization of a $10^{47} \times 10^{47}$ matrix exceeds what is computationally possible today by roughly 40 orders of magnitude!

It can be argued that determinants that differ from the ground state determinant only by a few functions affect the energy more than n-fold excited determinants. Thus truncating the wave-function expansion, by including only all up to, for example, doubly excited determinants, the dimensionality of the problem can be drastically reduced. Such a truncation is not without problems, though. The calculated energy of two infinitely separated, non-interacting systems should equal the sum of the two separate systems. This important property of the energy is called

size consistency. A related, more general, property of the energy has to do with the scaling of the energy with the number of electrons. The quality of the energy should be independent of the number of electrons. This property is usually referred to as size extensivity [34, 35]. When the wave-function expansion is indiscriminately truncated these two important properties are lost.

2.1.2   Perturbation theory

Perturbation theory is a very powerful technique for calculating corrections to the wave function and the energy of a known system. Suppose the complete eigenvalue spectrum of a Hamiltonian H_0 is known, and one wants to know the energy of the Hamiltonian $H = H_0 + \lambda H_1$, where $\{\lambda \in [0, 1]\}$ is an order parameter, which smoothly turns the perturbation on. When the effect of H_1 on the energy is small compared to H_0, H_1 can be treated as a perturbation to the Hamiltonian. When the solution to H is close to the unperturbed solution, the eigenvalues and eigenfunctions of H can be found by expanding both the energy and wave function in a series in λ:

$$(H_0 + \lambda H_1)(\Psi_n^{(0)} + \lambda \Psi_n^{(1)} + \lambda^2 \Psi_n^{(2)} + \ldots) =$$
$$(E_n^{(0)} + \lambda E_n^{(1)} + \lambda^2 E_n^{(2)} + \ldots)(\Psi_n^{(0)} + \lambda \Psi_n^{(1)} + \lambda^2 \Psi_n^{(2)} + \ldots). \quad (2.21)$$

Collecting terms in orders of λ and rearranging gives

$$E_n^{(0)} = \langle \Psi_n^{(0)} | H_0 | \Psi_n^{(0)} \rangle \qquad (2.22\text{a})$$
$$E_n^{(k)} = \langle \Psi_n^{(0)} | H_1 | \Psi_n^{(k-1)} \rangle \qquad (2.22\text{b})$$

The first-order energy correction can be calculated as a simple expectation value using the unperturbed zero-order wave function. The second-order energy, however, requires knowledge of the first-order perturbed wave function. Using the complete set of eigenfunctions of the unperturbed Hamiltonian, the perturbed wave function can be expanded in the set of eigenfunctions

$$\Psi_n^{(k)} = \sum_i c_{ni}^{(k)} \Psi_i^{(0)}. \qquad (2.23)$$

From Eq. 2.21, equations for the expansion coefficients $c_{ni}^{(1)}$ for the first-order correction to the wave function can be derived

$$c_{ni}^{(1)} = \frac{\langle \Psi_n^{(0)} | H_1 | \Psi_i^{(0)} \rangle}{E_n^{(0)} - E_i^{(0)}} \qquad (2.24)$$

The second-order energy expression is then

$$E_n^{(2)} = \sum_{i \neq n} \frac{\langle \Psi_n^{(0)} | H_1 | \Psi_i^{(0)} \rangle \langle \Psi_i^{(0)} | H_1 | \Psi_n^{(0)} \rangle}{E_n^{(0)} - E_i^{(0)}}. \qquad (2.25)$$

Using many-body perturbation theory it is possible to recover the correlation energy, order by order. The special case of perturbation theory, where the ground state wave function is a Hartree–Fock wave function, and the perturbation is the fluctuation potential, $H_1 = \sum_{i<j} r_{ij}^{-1} - \sum_i v^{HF}(i)$, is called Møller-Plesset (MP) perturbation theory. Expanding the perturbed wave function using excited determinants, and making use of Slater's rules for two-electron integrals, gives for the second-order correction to the ground-state energy

$$E_0^{(2)} = \frac{1}{4} \sum_{ijab} \frac{|\langle ij||ab \rangle|^2}{\epsilon_i + \epsilon_j - \epsilon_a - \epsilon_b}. \qquad (2.26)$$

Assuming that the perturbation series is convergent [36], more of the correlation energy can be recovered by progressively including higher order terms. The MP series can be shown to be both size consistent and size extensive [37].

2.1.3   Coupled-cluster theory

An alternative way of truncating the wave function, which retains both size consistency and size extensivity, is the so called coupled-cluster expansion (for a nice overview see [38] and references therein). A cluster function correlates two or more electrons, or more precisely, two or more orbitals, since electrons are indistinguishable. A cluster function correlating electrons in orbitals i and j can be written $f_{ij}(\mathbf{r}_p, \mathbf{r}_q) = \sum_{ab} t_{ij}^{ab} \phi_a(\mathbf{r}_p) \phi_b(\mathbf{r}_q)$, where a and b refer to virtual orbitals, and the t_{ij}^{ab} are the cluster amplitudes. A four-electron wave function, correlating the electrons in orbitals i and j would then be $\Psi = |(\phi_i \phi_j + f_{ij}) \phi_k \phi_l\rangle$. Clearly, to treat all electrons on an equal footing one should include the cluster functions for all other unique pairs, and also products of cluster functions, and even "one electron" clusters. One need not stop at pair-wise clusters; three-electron and higher order clusters can also be included.

Generating all possible and unique combinations of clusters quickly becomes very difficult as the number of electrons and basis functions increase. By using the formalism of second quantization, operators can be constructed which generate the cluster functions from a reference function. For example, the $\hat{t}_i = \sum_a t_i^a a_a^\dagger a_i$ operator generates the i:th single electron cluster function, $\hat{t}_{ij} = \sum_{ab} t_{ij}^{ab} a_a^\dagger a_b^\dagger a_i a_j$, generates a two-particle cluster function and so on. Thus, all single excitations can be generated by summing over all occupied orbital indices, $\hat{T}_1 = \sum_i \hat{t}_i$, and similarly for higher-order excitations. The coupled-cluster ansatz for the wave functions is then taken to be

$$\Psi_{CC} = e^{\hat{T}_1 + \hat{T}_2 + \cdots} \Psi_0 = e^{\hat{T}} |0\rangle. \tag{2.27}$$

By truncating the $\hat{T}$ operator at some excitation level, electron correlation is accounted for in a size-extensive manner. Including the operators up to the $\hat{T}_2$ operators gives to the so called CCSD method, and including $\hat{T}_3$ gives the CCSDT method. Although the $\hat{T}$ operator is formally truncated at some level, certain classes of higher order excitations are still included through products of lower-order excitations.

In practice it is beneficial to take a slightly different view on the wave function ansatz. Multiplying the Schrödinger equation from the left by the inverse of the exponential operator, and instead viewing the ansatz as a similarity transformed effective Hamiltonian, $W = e^{-T} H e^T$, leads to some substantial simplifications. Using the Baker-Campbell-Hausdorff (BCH)[37] series expansion the transformed Hamiltonian becomes

$$e^{-T} H e^T = H + [H, T] + \frac{1}{2!}[[H, T], T] + \frac{1}{3!}[[[H, T], T], T] + \dots, \tag{2.28}$$

where $[H, T]$ denotes the commutator between operators. Since the Hamiltonian contains at most two-body interactions, this infinite series truncates *exactly* at the fourth order, regardless of truncation of the T operator.

To obtain the coupled-cluster energy, one needs to solve the formal eigenvalue equation, $e^{-T} H e^T \Psi_0 = E \Psi_0$, where Ψ_0 is a reference wave function, typically a Hartree-Fock ground state determinant. Treating the energy equation as a normal eigenvalue problem is difficult, since the transformed Hamiltonian is non-Hermitian, and the $\hat{T}$ operator is unknown. Instead the coupled-cluster energy is calculated by left projection with the reference function, and the amplitudes are solved by projecting against the excited determinants.

$$\langle \Psi_0 | e^{-T} H e^T | \Psi_0 \rangle = E \tag{2.29}$$

$$\langle \Psi_{ij\dots}^{ab\dots} | e^{-T} H e^T | \Psi_0 \rangle = 0. \tag{2.30}$$

Using the similarity transformed Hamiltonian the energy- and amplitude equations are decoupled. The amplitude equations are non-linear and must be solved iteratively.

Solving the coupled-cluster equations is computationally very demanding. For example the CCSD method scales as $O(\mathcal{N}^6)$ with the system size. The CCSDT method scales as $O(\mathcal{N}^8)$, which quickly becomes intractable for larger molecules. The strength of the coupled-cluster methods is that they can consistently provide highly accurate results, both for the energy and properties,

for a wide range of molecular systems. The MP2 method, which has a formal scaling of $O(\mathcal{N}^5)$, does not provide the same level of accuracy and consistency. It can be shown that the initial step in a CCSD calculation gives the MP2 energy. As a side note, the formal scaling of both MBPT and CC methods can be reduced using various techniques, including density fitting [39, 40] and localization techniques [41, 42]. Today there exist CC and MBPT methods which scale linearly with the system size, however, sacrificing some of the accuracy [43, 44].

2.1.4 Density-functional theory

In 1964 Hohenberg and Kohn [45] showed that the wave function in fact contains a large degree of redundancy, and that only knowledge of the ground state electron density is needed to calculate the energy and corresponding molecular properties. Thus, instead of having to deal with a $3N$-dimensional wave function, every molecular ground-state property can be calculated from a quantity which is only 3-dimensional. This seemingly immense simplification relies on the existence of a functional of the density which gives the exact energy of the system. This functional is unfortunately not known, and one can only assume it to be as complicated as the wave function itself. There are thus two problems; obtaining the exact density of the system and finding the functional which gives the energy. By going back to wave mechanics it is possible to formulate equations for obtaining both the density and the energy. In the Kohn-Sham equations [46] the density is expanded in a basis of molecular orbitals, similar to the Hartree-Fock equations. The kinetic energy is taken to be the expectation value of the usual kinetic energy operator, and the Coulomb interactions are retained. The non-local exchange terms are strictly wave mechanical, arising from the antisymmetry of the *wave function*. The exchange *potential*, however, is a pure quantum effect, and cannot be neglected. In pure DFT, exchange is accounted for by introducing a *local* exchange functional of the density. The Kohn-Sham energy for a molecular system is

$$E_{KS} = \langle \hat{h} \rangle + J[\rho] + E_{xc}[\rho], \tag{2.31}$$

where square brackets have been used to indicate functionals, and E_{xc} is a functional which tries to account for electron exchange, parts of the kinetic energy and the effects electron correlation. In hybrid-DFT methods [47, 48], some exact Hartree–Fock exchange is included by scaling the HF exchange operator.

In principle Eq. 2.31 is exact, provided that the exact density is known, and that the exact form of E_{xc} is known. Much work has been done in the field of developing approximate functionals which can give accurate energies for a wide range of molecules, and modern DFT functionals are performing very well. In some respects DFT can be viewed as empirically corrected Hartree-Fock methods, but also *first principles* DFT methods exist [49, 50].

Computationally the DFT equations are solved in much the same way as the Hartree–Fock equations, and the computational scaling is similar or better. The scaling of DFT can be improved by using density fitting, also sometimes called resolution of the identity (RI), techniques [39, 51, 52, 53]. Since pure DFT lacks exact Hartree–Fock exchange (which is non-local), scaling can be improved by expanding the Coulomb operator in a fitting basis which reduces the two-electron integrals from four index to three index quantities. Using this technique the formal scaling of DFT can be reduced to $O(\mathcal{N}^3)$. It should be noted that similar techniques can be used to improve the scaling of other methods as well [40, 54, 55]. Techniques also exist for fitting of the exchange operator, but the overall gain in performance is not as significant as for the Coulomb operator [56]. The advantageous scaling of DFT, combined with, in many cases, the far superior accuracy compared to Hartree–Fock, has contributed to the immense popularity of DFT-based methods.

Chapter 3

Molecular properties as energy derivatives

Many molecular properties, arising from interactions with external fields (*e.g.* electric, magnetic) can conveniently be calculated using derivative theory [57]. When the field is weak, it can be considered as a small perturbation on the system. Most external fields are weak on the atomic scale, the exception being strong laser fields. The effect of the applied field on the molecular system can be calculated by expanding the energy in a Taylor series around a stationary point of the unperturbed system

$$E(\lambda) = E_0 + \lambda E^{(1)} + \lambda^2 E^{(2)} + \dots, \tag{3.1}$$

where $E^{(n)}$ is the n:th derivative of the energy with respect to the external perturbations

$$E^{(n)} = \frac{1}{n!} \frac{d^n E(\lambda)}{d\lambda^n}. \tag{3.2}$$

Depending on the perturbation, the different derivatives of the energy can be identified as measurable properties of the system.

To evaluate a property which depends, to first order, on λ, we need to calculate the first derivative of the energy with respect to the perturbation.

$$\left.\frac{dE(\lambda)}{d\lambda}\right|_{\mathbf{c}=\mathbf{c}'} = \left.\frac{\partial\mathcal{E}(\lambda;\mathbf{c})}{\partial\lambda}\right|_{\mathbf{c}=\mathbf{c}'} + \left.\frac{\partial\mathcal{E}(\lambda;\mathbf{c})}{\partial\mathbf{c}}\frac{\partial\mathbf{c}}{\partial\lambda}\right|_{\mathbf{c}=\mathbf{c}'}, \tag{3.3}$$

where $\mathcal{E}(\lambda;\mathbf{c}') = E(\lambda)$ when the wave-function coefficients $\mathbf{c}$ satisfies the stationary condition for $\mathbf{c} = \mathbf{c}'$

$$\left.\frac{\partial\mathcal{E}(\lambda;\mathbf{c})}{\partial\mathbf{c}}\right|_{\mathbf{c}=\mathbf{c}'} = 0. \tag{3.4}$$

The first term on the right hand side of Eq. 3.3 represents the effect of the perturbation while keeping the wave function unaltered. The second term represents the energy change as the electrons adjusts themselves to the perturbed environment [58]. The second term is usually called the relaxation or response term. However, due to the stationary condition (Eq. 3.4) the second term in Eq. 3.3 vanishes. This result is equivalent to the Hellmann-Feynman theorem

$$\frac{\partial}{\partial\lambda}\langle\Psi|H|\Psi\rangle = \langle\Psi|\frac{\partial H}{\partial\lambda}|\Psi\rangle, \tag{3.5}$$

which holds for both exact and variationally optimized wave functions. A similar condition also exists for coupled-cluster wave functions [59]. Thus, to calculate first-order properties no information about the orbital relaxation is needed. However, in case the wave-function parameterization depends explicitly on the perturbation, the Hellmann–Feynman theorem is not valid. This is typically the case for geometric perturbations, and for field-dependent basis functions commonly used in conjunction with calculations of magnetic properties.

For second-order properties, we need to evaluate the second derivative of the energy with respect to the perturbation

$$\left.\frac{d^2 E(\lambda)}{d\lambda^2}\right|_{\mathbf{c}=\mathbf{c}'} = \left.\frac{\partial^2 \mathcal{E}(\lambda; \mathbf{c})}{\partial\lambda^2}\right|_{\mathbf{c}=\mathbf{c}'} + \left.\frac{\partial^2 \mathcal{E}(\lambda; \mathbf{c})}{\partial\lambda\partial\mathbf{c}}\frac{\partial\mathbf{c}}{\partial\lambda}\right|_{\mathbf{c}=\mathbf{c}'}. \tag{3.6}$$

The last term in Eq. 3.6 involves the derivatives of the expansion coefficients with respect to the perturbation. Equations for these response terms are obtained by differentiating the stationary condition Eq. 3.4 with respect to the perturbation

$$\left.\frac{d}{d\lambda}\frac{\partial \mathcal{E}(\lambda; \mathbf{c})}{\partial\mathbf{c}}\right|_{\mathbf{c}=\mathbf{c}'} = \left.\frac{\partial^2 \mathcal{E}(\lambda; \mathbf{c})}{\partial\lambda\partial\mathbf{c}}\right|_{\mathbf{c}=\mathbf{c}'} + \left.\frac{\partial^2 \mathcal{E}(\lambda; \mathbf{c})}{\partial\mathbf{c}^2}\frac{\partial\mathbf{c}}{\partial\lambda}\right|_{\mathbf{c}=\mathbf{c}'} = 0. \tag{3.7}$$

The response terms describe the changes to the wave function which make it stationary in the presence of the perturbation. Introducing the following notations for the electronic gradient

$$\boldsymbol{\mathcal{F}}(\lambda) = \frac{\partial \mathcal{E}(\lambda; \mathbf{c})}{\partial\mathbf{c}}, \tag{3.8}$$

and the electronic Hessian

$$\boldsymbol{\mathcal{G}}(\lambda) = \frac{\partial^2 \mathcal{E}(\lambda; \mathbf{c})}{\partial\mathbf{c}^2}, \tag{3.9}$$

Eq. 3.7 can be written as Newton's equation

$$\boldsymbol{\mathcal{G}}(\lambda)\frac{\partial\mathbf{c}}{\partial\lambda} = -\frac{\partial\boldsymbol{\mathcal{F}}(\lambda)}{\partial\lambda}. \tag{3.10}$$

This set of equations can be solved by calculating the inverse of the Hessian. In practice this is usually not feasible due to the size of the Hessian matrix, which formally has a dimension of $N^2 \times N^2$, where N is the number of basis functions.

3.1 Coupled Hartree-Fock theory

Perhaps the most elegant way to obtain practical equations for the response vectors, is to explore the fact that the change in the wave function due to the perturbation must be such that the Brillouin condition is restored. The Brillouin condition states that the ground-state Hartree–Fock wave function is orthogonal to all singly excited determinants [60]. Differentiation of the Brillouin condition, together with the orthonormality condition yields a set of explicit equations for the response vectors [61]. Here, I will follow a different derivation, which retains a closer relationship to the wave function [32]. In order to keep the equations simple an orthogonal basis is assumed.

Changes to the wave function which preserve orthonormality, can be parameterized using an orbital rotation operator $e^{\boldsymbol{\kappa}}$, where $\boldsymbol{\kappa}$ is an anti-hermitian matrix $\boldsymbol{\kappa}^\dagger = -\boldsymbol{\kappa}$. The $\boldsymbol{\kappa}$ matrix can be expressed in terms of annihilation and creation operators

$$e^{\boldsymbol{\kappa}} = \exp\left(\sum_{ia} \kappa_{ia} a_a^\dagger a_i\right) = 1 + \boldsymbol{\kappa} + \frac{\boldsymbol{\kappa}^2}{2} + \ldots, \tag{3.11}$$

where the summation is restricted to the occupied-virtual space*. Operating on the reference wave function with the orbital rotation operator gives

$$\Psi_0' = \Psi_0 + \sum_{ia} \kappa_{ia}\Psi_i^a + \sum_{ijab} \kappa_{ia}\kappa_{ib}\Psi_{ij}^{ab} + \ldots. \tag{3.12}$$

---

*The Hartree–Fock energy is invariant to orbital rotations within the occupied-occupied and virtual-virtual spaces.

Taking the first and second order derivatives with respect to the orbital rotation parameters, in the limit of $\boldsymbol{\kappa} = 0$, yields

$$\frac{\partial \Psi_0}{\partial \kappa_{ia}} = \Psi_i^a \tag{3.13}$$

$$\frac{\partial^2 \Psi_0}{\partial \kappa_{ia} \partial \kappa_{jb}} = (1 - \delta_{ij}) \Psi_{ij}^{ab}. \tag{3.14}$$

The energy derivatives in Equations 3.8 and 3.9 can now be evaluated. Using Slater's rules, the expression for the gradient is (ignoring complex conjugates)

$$\frac{\partial \langle \Psi_0 | H | \Psi_0 \rangle}{\partial \kappa_{ia}^*} = \langle \Psi_i^a | (H - E) | \Psi_0 \rangle = \langle a | h | i \rangle + \sum_j \langle aj || ij \rangle = \langle a | F | i \rangle. \tag{3.15}$$

The electronic gradient can thus be obtained from the off-diagonal elements of the Fock matrix. For a variationally optimized wave function, all off-diagonal elements of the Fock matrix are zero in the canonical representation, and the gradient vanishes. The previous equation is also a proof of the Brillouin condition [60]. Although the gradient is zero for an optimized wave function, this is not necessarily the case when the perturbation is turned on, $H \to H + H_1, H_1 = \sum_i h_i'(\lambda)$. For the Hessian we get two terms

$$\frac{\partial^2 \langle \Psi_0 | H | \Psi_0 \rangle}{\partial \kappa_{ia}^* \partial \kappa_{jb}^*} \quad = \langle \Psi_{ij}^{ab} | (H - E) | \Psi_0 \rangle \quad = \langle ab || ij \rangle \tag{3.16}$$

$$\frac{\partial^2 \langle \Psi_0 | H | \Psi_0 \rangle}{\partial \kappa_{ia}^* \partial \kappa_{jb}} \quad = \langle \Psi_i^a | (H - E) | \Psi_j^b \rangle \quad = \delta_{ij} \delta_{ab} (\epsilon_a - \epsilon_i) + \langle ai || jb \rangle. \tag{3.17}$$

In an orthonormal basis, the equations for the response vectors, $\partial \mathbf{c} / \partial \lambda = \mathbf{U}$ from Eq. 3.10 for a perturbation $h'(\lambda)$ are

$$\langle a | h'(\lambda) | i \rangle + \sum_{jb} [\delta_{ij} \delta_{ab} (\epsilon_a - \epsilon_i) + \langle ai || jb \rangle U_{ai}] + \sum_{jb} \langle ab || ij \rangle U_{ai}^* = 0. \tag{3.18}$$

U_{ai} are thus the sought coefficients that describe the orbital rotations that make the energy stationary in the presence of the perturbation. In practice one prefers to work in a non-orthonormal basis, as all integrals would have to be transformed from the AO basis to the MO basis

$$\langle ij | kl \rangle = \sum_{\mu\nu\sigma\lambda} C_{\mu i} C_{\nu j} C_{\sigma k} C_{\lambda l} \langle \mu\nu | \lambda\sigma \rangle, \tag{3.19}$$

which has a very unfavorable computational scaling of $O(\mathcal{N}^5)$.

When the wave function is explicitly dependent on the perturbation through the basis functions, the response equations become slightly more complicated [58, 62, 63, 64, 65]. The occupied-virtual blocks are given by

$$\sum_{em} [\langle am || ie \rangle - \langle ae || im \rangle + \delta_{im} \delta_{ea} (\epsilon_a - \epsilon_i)] U_{em} =$$

$$- \sum_{\mu\nu} c_{\mu a}^* \left(\frac{\partial h_{\mu\nu}}{\partial \lambda} + \sum_m \sum_{\sigma\rho} c_{\sigma m}^* c_{\rho m} \frac{\partial \langle \mu\sigma || \nu\rho \rangle}{\partial \lambda} \right) c_{\nu i} + \sum_{mn} S_{mn}^\lambda \langle an || im \rangle + S_{ai}^\lambda \epsilon_a, \tag{3.20}$$

where S_{nm}^λ represents the AO overlap matrix differentiated with respect to the perturbation

$$S_{\mu\nu}^\lambda = \frac{\partial \langle \mu | \nu \rangle}{\partial \lambda}, \tag{3.21}$$

and rotated back to the MO representation. The occupied-occupied and virtual-virtual blocks can be determined from the orthonormality condition $U_{pq} + S_{pq} + U_{qp}^* = 0$.

Knowledge of the response vectors $\mathbf{U}$ allows us to construct the perturbed density matrix for the perturbation λ

$$\frac{\partial D_{\mu\nu}}{\partial \lambda} = \sum_{pi}(U_{pi}^* c_{\mu p}^* c_{\nu i} + c_{\mu i}^* c_{\nu p} U_{pi}), \qquad (3.22)$$

which we shall need later (see Sec. 6.2).

The same ideas as outlined above can also be used when electron correlation is taken into account at coupled-cluster or perturbation-theory levels. The treatment gets somewhat more involved, as the density matrices are replaced by effective or "relaxed" electron densities. The relaxed densities can be determined via the solution of the so called Z-vector equations [66], and the corresponding derivatives of the densities are obtained by differentiating the zeroth-order Z-vector equations [62].

Chapter 4

Magnetic interactions in closed-shell molecules

When a molecule is subjected to an external magnetic field, the electrons respond by reorganizing in order to minimize the effect on the energy caused by the field. One of the main effects of the magnetic field is to induce currents in the molecule. The current induces a secondary magnetic field which, in most molecules, opposes the external field, thereby minimizing the effect of the external field. This phenomenon is in many ways similar to classical electrodynamics, where an oscillating magnetic field induces a diamagnetic current in a conductor. There are however differences. In molecules, a static magnetic field can induce a current which persists until the magnetic field is turned off. This phenomenon is not related to superconductivity, however, since superconductivity is a solid state or bulk property. In molecules the electrons move in energetically discrete states, so that no scattering occurs and hence there is no resistance.

In closed-shell molecules the total electronic orbital angular momentum $\mathbf{L}$ and total spin angular momentum $\mathbf{S}$ are zero. In other words, there are no net intrinsic magnetic moments arising from the electrons in the system. However, an external magnetic field can couple with the individual angular momenta and spins of the electrons. The coupling of electrons with magnetic fields also induce currents, $\mathbf{J}$, which in turn give rise to additional magnetic fields. Nuclei with spin $I > 0$ also carry an intrinsic magnetic moment. The nuclear magnetic moments can interact with each other, giving rise to direct, anisotropic spin-spin coupling between the nuclei. The nuclear spins also couple with an external magnetic field, which is the basis for nuclear magnetic resonance (NMR) spectroscopy. The nuclear spins can also couple indirectly through the electron spin and orbital angular momenta, giving rise to indirect spin-spin coupling, which is of great analytic importance in NMR spectroscopy. Furthermore, there are other magnetic interactions in molecules. These are due to non-adiabatic corrections, *i.e.* due to the Born–Oppenheimer (see Chap. 2) approximation not being exact. These interactions, described by the rotational and vibrational g-tensors, give rise to small splittings in rotational and vibrational spectra [67].

In this section I will focus on the interaction between electrons and an external magnetic field.

4.1 The magnetically induced probability current

Although we shall only be concerned with time-independent phenomena, the time-dependent Schrödinger equation

$$\hat{H}\Psi(\mathbf{r},t) = -i\frac{\partial}{\partial t}\Psi(\mathbf{r},t) \tag{4.1}$$

is needed to derive an expression for the current. Differentiating the time-dependent density

$$\rho(\mathbf{r},t) = N \int_{-\infty}^{\infty} d\mathbf{r}_2...d\mathbf{r}_N |\Psi(\mathbf{r},\mathbf{r}_2,...\mathbf{r}_N,t)|^2, \tag{4.2}$$

with respect to the time coordinate gives together with Eq. 4.1 the continuity equation

$$\frac{\partial}{\partial t}\rho(\mathbf{r}, t) = -\nabla \mathbf{J}(\mathbf{r}, t), \tag{4.3}$$

where $\mathbf{J}(\mathbf{r}, t)$ is the flux, or the probability current

$$\mathbf{J}(\mathbf{r}, t) = \frac{1}{2i} \int_{-\infty}^{\infty} d\mathbf{r}_2...d\mathbf{r}_N (\Psi^* \nabla \Psi - \nabla \Psi^* \Psi). \tag{4.4}$$

When the wave function is real, and the system is independent of time, the current must vanish. Equation 4.3 represents a conservation law; a change in the density in some region must be compensated by a flux in or out of that region.

The magnetic field is introduced into the quantum mechanical framework through minimal substitution of the magnetic vector potential, $\mathbf{A}$, into the kinetic energy operator

$$\mathbf{p} \to \boldsymbol{\pi} = \mathbf{p} + \frac{e}{c}\mathbf{A}, \tag{4.5}$$

where $\mathbf{p} = -i\nabla$, e is the electron charge and c is the speed of light*. It is possible to show that this gives the correct form for the Hamiltonian by considering the Lagrangian for the Lorentz force of a electron in an electromagnetic field [68]. The vector potential itself is related to the magnetic field through the relation $\mathbf{B} = \nabla \times \mathbf{A}$.

The magnetic vector potential of interest consists of two contributions, $\mathbf{A} = \mathbf{A^B} + \mathbf{A^{m_I}}$. The first term describes a uniform, time-independent external magnetic field

$$\mathbf{A^B}(\mathbf{r}) = \frac{1}{2}\mathbf{B} \times (\mathbf{r} - \mathbf{R}_O), \tag{4.6}$$

where $\mathbf{R}_O$ is the chosen origin of the magnetic field. The second term is due to the magnetic moments of the nuclei

$$\mathbf{A^{m_I}}(\mathbf{r}) = \sum_I \mathbf{m}_I \times \frac{\mathbf{r} - \mathbf{R}_I}{|\mathbf{r} - \mathbf{R_I}|^3}, \tag{4.7}$$

where $\mathbf{m}_I$ is the magnetic moment of the Ith nucleus, and $\mathbf{R}_I$ the nuclear position vector.

In the presence of a uniform, time-independent magnetic field the probability current is

$$\mathbf{J}(\mathbf{r}) = \frac{i}{2} \int d\mathbf{r}_2..d\mathbf{r}_N \left(\Psi^* \nabla \Psi - \Psi \nabla \Psi^* + \frac{2i}{c}\mathbf{A}\Psi^*\Psi \right). \tag{4.8}$$

Due to the last term, which involves the electronic density, the current is non-vanishing in the presence of a magnetic field. Furthermore, the other two terms are no longer necessarily zero, either. The wave function is implicitly dependent on the magnetic field, as well as complex. The first order change in the wave function due to the magnetic field can be expressed using a series expansion

$$\Psi = \Psi_0^{(0)} + \Psi_0^{(1)} + \ldots = \Psi_0 + \frac{\partial \Psi_0}{\partial \mathbf{B}}\mathbf{B} + \ldots \tag{4.9}$$

Inserting Eq. 4.9 into Eq. 4.8 yields

$$\mathbf{J}(\mathbf{r}) = \frac{i}{2} \int d\mathbf{r}_2..d\mathbf{r}_N \left[\left(\Psi_0^{(1)*}\nabla\Psi_0 + \Psi_0^*\nabla\Psi_0^{(1)} - \Psi_0^{(1)}\nabla\Psi_0^* - \Psi_0\nabla\Psi_0^{(1)*} \right)\mathbf{B} + \frac{2i}{c}\mathbf{A}\Psi_0^*\Psi_0 \right]. \tag{4.10}$$

The last term in Eq. 4.10 is commonly referred to as the diamagnetic contribution, and the other terms are collectively known as the paramagnetic contribution to the current. This terminology can be somewhat confusing, since the particular choice of the gauge, affects both the size and the sign of the two contributions, leaving only the sum invariant. Only atoms have a natural gauge origin at the nucleus, which annihilates the paramagnetic terms for closed-shell atoms.

---
*In atomic units $c = 137.035987$.

The first-order perturbed wave function $\Psi_0^{(1)}$ can be obtained by solving the Coupled-Perturbed Hartree–Fock equations for a magnetic perturbation.

The induced current has to obey the law of charge conservation which states that in an isolated system charge can not be created nor destroyed. Charge conservation is not a property which is imposed on the equations, rather a condition that must be fulfilled. For a molecule in a stationary state the charge-conservation condition becomes $\nabla \cdot \mathbf{J} = 0$, in any point of space. Alternatively this can be stated in terms of the Sambe-Epstein integral condition [69]

$$\int \mathbf{J}(\mathbf{r}) \cdot d\mathbf{r} = 0. \tag{4.11}$$

For closed-shell molecules in the absence of an external magnetic field, Eq. 4.11 reduces to $\mathbf{J} = \mathbf{0}$.

The induced current gives rise to a secondary magnetic field. The strength of the induced magnetic field can be calculated using the Biot-Savart law

$$\mathbf{B}(\mathbf{r}) = \frac{1}{c} \int \frac{\mathbf{J}(\mathbf{r}) \times \mathbf{r}_I}{|\mathbf{r}_I|^3}. \tag{4.12}$$

Inserting Eq. 4.8 into the Biot-Savart equation, gives an expression for the internal magnetic field at a nucleus in a molecule

$$\mathbf{B}_{\text{int}} = -\frac{1}{2c^2}\langle\Psi|\frac{\mathbf{A} \times \mathbf{r}_I}{|\mathbf{r}_I|^3}|\Psi\rangle + \frac{i\mathbf{B}}{c}\langle\frac{\partial\Psi}{\partial\mathbf{B}}|\frac{\mathbf{r}_I \times \nabla}{|\mathbf{r}_I|^3}|\Psi\rangle + \frac{i\mathbf{B}}{c}\langle\Psi|\frac{\mathbf{r}_I \times \nabla}{|\mathbf{r}_I|^3}|\frac{\partial\Psi}{\partial\mathbf{B}}\rangle. \tag{4.13}$$

Making the identification

$$\frac{\partial H}{\partial\mathbf{m}_I} = -\frac{i}{c}\frac{\mathbf{r}_I \times \nabla}{|\mathbf{r}_I|^3} \tag{4.14}$$

$$\frac{\partial^2 H}{\partial\mathbf{m}_I\partial\mathbf{B}} = \frac{i}{2c^2}\frac{(\mathbf{r}_I \cdot \mathbf{r}_O)\mathbf{1} - \mathbf{r}_I\mathbf{r}_O}{|\mathbf{r}_I|^3}, \tag{4.15}$$

gives

$$\mathbf{B}_{\text{int}} = -\frac{\partial^2 E}{\partial\mathbf{m}_I\partial\mathbf{B}}\mathbf{B} = -\sigma_I\mathbf{B}, \tag{4.16}$$

which is the definition of the nuclear magnetic shielding tensor, σ_i. In terms of the energy expression in Eq. 2.12, the second derivative expression for the nuclear magnetic shielding becomes

$$\sigma_{\alpha\beta} = \sum_{\mu\nu} D_{\mu\nu}\frac{\partial^2 h_{\mu\nu}}{\partial m_\alpha^I \partial B_\beta} + \sum_{\mu\nu}\frac{\partial D_{\mu\nu}}{\partial B_\beta}\frac{\partial h_{\mu\nu}}{\partial m_\alpha}. \tag{4.17}$$

4.2 The gauge problem

The magnetic field defined by $\mathbf{B} = \nabla \times \mathbf{A}$ is unique, but the vector potential itself is not. The relation contains a hidden ambiguity arising from the fact that the curl of any gradient vanishes: $\nabla \times \nabla\lambda(\mathbf{r}) = \mathbf{0}$ for an arbitrary scalar function $\lambda(\mathbf{r})$. Thus, addition of the gradient of a scalar function to the vector potential leaves the magnetic field unchanged. To a given magnetic field there are an infinite number of vector potentials. Such an addition can be viewed as a change of the gauge origin of the vector potential. As a consequence of the translational invariance of space the energy of any system must be invariant to the choice of gauge.

In general, transformations which leave the energy invariant are represented by unitary transformations. It can be shown that a gauge transformation of the vector potential

$$\mathbf{A}(\mathbf{r}) \rightarrow \mathbf{A}'(\mathbf{r}) = \mathbf{A}(\mathbf{r}) + \nabla\Lambda(\mathbf{r}), \tag{4.18}$$

is equivalent to a unitary transformation of the Hamiltonian

$$\mathbf{H}(\mathbf{A}') = e^{-i\Lambda}\mathbf{H}(\mathbf{A})e^{i\Lambda}. \tag{4.19}$$

A typical gauge transformation is

$$\mathbf{A}(\mathbf{r}) \rightarrow \mathbf{A}'(\mathbf{r}) = \frac{1}{2}\mathbf{B} \times \mathbf{r} + \frac{1}{2}\nabla(\mathbf{B} \times \mathbf{d} \cdot \mathbf{r}) = \frac{1}{2}\mathbf{B} \times (\mathbf{r} + \mathbf{d}), \qquad (4.20)$$

which displaces the gauge origin by the vector $\mathbf{d}$. Under the transformation the wave function has to change correspondingly, so that the original wave function is related to the new wave function by a phase factor

$$\mathbf{\Psi}(\mathbf{A}') = e^{-i\Lambda}\mathbf{\Psi}(\mathbf{A}), \qquad (4.21)$$

where $\Lambda = \mathbf{B} \times \mathbf{d} \cdot \mathbf{r}$.

It can be shown, using the hypervirial theorem

$$\langle \Psi(\mathbf{A})|[\Lambda, \hat{H}(\mathbf{A})]|\Psi(\mathbf{A})\rangle = 0, \qquad (4.22)$$

that charge conservation is in fact equivalent to gauge invariance [70]. More generally, charge conservation is a consequence of the Nöther theorem [71], which connects conserved quantities to symmetries of nature.

It can be shown that exact solutions to the Schrödinger equation are gauge invariant [68]. Certain approximate solutions to the Schrödinger equation can also be shown to be gauge invariant. Most importantly, energies calculated from variationally optimized wave functions are gauge invariant when the following conditions hold: The set of optimal trial functions are invariant to the set of gauge transformations $\exp(-i\Lambda)$, and using this same set of trial functions with both $H(A)$ and $H(A')$ the resulting wave functions are related through Eq. 4.21 and give the same energies. All variationally optimized wave functions do not give gauge invariant energies, though. Uncoupled Hartree-Fock theory is not gauge invariant, but the coupled Hartree-Fock equations are, due to the relaxation of the wave function [72]. Non-variational methods like Møller-Plesset perturbation theory and coupled-cluster theory do not exactly fulfill the hypervirial theorem in Eq. 4.22. Despite not being formally gauge invariant, the inherent gauge error of these methods is significantly smaller than the gauge error introduced by truncating basis set [62, 73] (*vide infra*).

4.2.1   The gauge problem in a finite basis

Although certain approximate solutions to the Schrödinger equation can be shown to be formally gauge invariant, this invariance only holds in the limit of an infinite basis. The reasons behind this problem can be understood in a number of ways. It is illuminating to consider an alternative expression to Eq. 4.17 for the nuclear magnetic shielding tensor derived from perturbation theory

$$\sigma_I = \langle 0|\hat{h}_I^{dia}|0\rangle - 2\sum_{n \neq 0}\frac{\langle 0|\hat{l}_O|n\rangle\langle n|(\hat{h}_I^{pso})^T|0\rangle}{E_n - E_0}, \qquad (4.23)$$

with

$$\hat{h}^{dia} = \frac{(\mathbf{r}_O \cdot \mathbf{r}_I)\mathbf{1} - \mathbf{r}_O\mathbf{r}_I}{r_I^3} \qquad (4.24\text{a})$$

$$\hat{h}^{pso} = \frac{(\mathbf{r} - \mathbf{r}_I) \times \mathbf{p}}{r_I^3} \qquad (4.24\text{b})$$

$$\hat{l}_O = (\mathbf{r} - \mathbf{r}_O) \times \mathbf{p}, \qquad (4.24\text{c})$$

where $\mathbf{r}_I$ is the coordinate of the Ith nucleus and $\mathbf{r}_O$ is the point where $\hat{l}_O$ vanishes. The convergence of Eq. 4.23 in a finite basis depends largely on the convergence of the matrix representation of the angular momentum operator $\hat{l}_O$. The dependence of $\hat{h}^{dia}$ and $\hat{h}^{pso}$ on the basis set is a lot less severe due to the nuclei centered basis functions and the r^{-3} dependence of these operators, making them inherently local. Considering an atom, which has a natural gauge origin at the nucleus, and the wave function is an eigenfunction of the angular momentum operator, it can be shown that a gauge transformation results in a truncation of the representation of the operator

which is different depending on the gauge [61]. The further away from the nucleus the origin is, the worse the representation becomes. Molecules do not have a natural gauge origin. With the exception of linear molecules, the wave function is not an eigenfunction to any component of the angular momentum operator. The lack of eigenfunctions also implies that there exists no natural basis in which to expand the operator.

An alternative way of viewing the gauge problem is to focus on the unitary gauge transformation operators $U = \exp(-i\lambda(\mathbf{r}))$. The matrix representation of these operators, in a finite basis, is not exactly unitary. This can be seen if one expands the operators in a Taylor series

$$e^{-i\lambda(\mathbf{r})} = 1 - i\lambda(\mathbf{r}) + \lambda^2(\mathbf{r}) - \dots, \qquad (4.25)$$

where $\lambda(\mathbf{r}) = \frac{1}{2}\nabla\mathbf{B} \times \mathbf{d} \cdot \mathbf{r}$ (using the definition in Eq. 4.20). The effect of this operator on an infinite basis can be rationalized in the following way. Focusing on the second term in Eq. 4.25, it will essentially transform the basis functions as follows (assuming λ is linear in r): $s \rightarrow p$, $p \rightarrow d$, ..., *i.e.* it increments the l quantum number of the basis functions. In an infinite basis this corresponds to a change of the linear expansion coefficients. In a finite basis, however, the operator effectively changes the space *spanned* by the basis, and hence the original and transformed functions are no longer related by a unitary transformation. As a result, exact gauge invariance is no longer fulfilled [68, 70].

A number of different approaches exists that try to remedy the gauge invariance problem in a finite basis set representation. None of these approaches accomplishes true gauge invariance, but rather gauge-origin independence. Two very similar approaches, the methods of Localized Orbitals for Local Origins (LORG) by Bouman and Hansen [74], and the Individual Gauges for Localized Orbitals (IGLO) by Kutzelnigg [75] address the problem by localizing the molecular orbitals and applying gauge transformations to the individual localized molecular orbitals. One problem with these approaches is that localization of the orbitals is an iterative process which can be very slow, and sometimes even impossible for systems where the electrons are truly delocalized. Although these approaches work very well, and improve basis set convergence significantly, it has proved difficult to generalize them from the Hartree-Fock framework to electron correlated methods, although some such methods have been developed [76, 77].

4.2.2   Gauge-including atomic orbitals

An elegant way of dealing with the gauge problem is through the use of explicitly field-dependent basis functions. First proposed by London in 1937 [78], the so called London orbitals or Gauge-Including Atomic Orbitals (GIAOs) are defined as

$$\chi_\mu(\mathbf{r}) = e^{-\frac{i}{2c}(\mathbf{B}\times[\mathbf{R}_\mu - \mathbf{R}_O]\cdot\mathbf{r})}\chi_\mu^{(0)}(\mathbf{r}), \qquad (4.26)$$

where $\chi_\mu^{(0)}(\mathbf{r})$ denotes a standard Gaussian-type basis function with $\mathbf{R}_\mu$ as center, and $\mathbf{R}_O$ is the chosen gauge origin. The GIAO is thus a gauge transformed atomic orbital, with the new gauge origin at the nucleus. One justification for the use of GIAOs is, that they are correct to first order for the atomic problem in a magnetic field. Using the same arguments as for the LCAO approximation, the GIAO seems quite natural; the GIAOs extend the basis so that the expansion of the operators in Eq. 4.23 converges faster. Appealing as such an interpretation might be, it provides very little insight into the actual effect of the GIAOs. The GIAOs are better viewed as gauge transformations of the individual basis functions. Since the AOs are inherently local, such a transformation has only a local effect, ensuring an optimal gauge for the AOs. The use of GIAOs eliminates any explicit reference to the global gauge origin $\mathbf{R}_O$ in the expressions for the nuclear magnetic shielding constants and other magnetic properties [79]. It is important to keep in mind that the GIAOs are not proper gauge transformations of the wave function, nor of the molecular orbitals and their use does not make the energy gauge invariant. GIAOs do, however, ensure rapid basis-set convergence for many second-order magnetic properties, and thus resolve the gauge problem.

There are a number of complications with the use of GIAOs, which hampered their use for quite a while. The first problem is due to the explicit field dependence in the basis which complicates the expressions for magnetic properties. GIAOs were first used in nuclear magnetic shielding calculations by Pople[80, 81] and Hameka [82], and later popularized by Ditchfield and others [83, 84, 85]. One of the main problems was the calculation of integrals involving GIAOs. The actual breakthrough of the GIAO approach is due to the work of Wolinski *et al.* [86, 87] who demonstrated that modern analytic derivative theory [88] can be efficiently used for the calculation of nuclear magnetic shieldings within the GIAO framework. The GIAO approach has since then been implemented in most of the popular quantum chemical program systems [89, 90, 91] and also been extended to post-Hartree–Fock, multi-configuration and DFT methods [92, 93, 94, 95, 96, 97, 98, 99, 100, 101, 102, 103, 104, 105].

Chapter 5

Ring currents and aromaticity

Aromaticity is a property used to describe certain cyclic molecules, possessing some "unusual" properties. Although aromatic molecules have been known for more than 150 years, no one has yet been able to exactly and quantitatively determine what aromaticity is. In many respects, aromaticity is an experimentalist's finger-tip classification of molecules which possess some special properties. Such properties are high stability and low reactivity, site specific reactions, reduced bond length alternation, high magnetizability and "aromatic smell". Common structural denominators for these molecules are that they are cyclic, planar and have conjugated double bonds. Not all molecules fulfilling these criteria are aromatic, and there are molecules which are considered aromatic but are not planar nor conjugated in the normal sense. Apart from the structural requirements, there is also an electronic prerequisite that the conjugated ring occupies $(4n + 2)$ π-electrons. This rule was discovered by Hückel [106, 107], and although this rule is not strict, it holds remarkably well. The origins of this rule can be understood when one considers a symmetric, simplified cyclic system with one π-orbital at each center. The nodal structure of the Hückel molecular orbitals constructed from these orbitals has the following general pattern (Fig. 5.1): The MO with the lowest energy has no nodal plane, the two following MOs have one nodal plane, and are degenerate. When the system has an odd number of orbitals all higher orbitals come in degenerate pairs. On the other hand, if the system has an even number of orbitals, the highest energy orbital is not degenerate and all orbitals between the highest and lowest are pairwise degenerate. Stated in another way; the angular part of a wave function in a circular potential would correspond to $\Psi(\theta) = e^{i|m|\theta}$, where $\{m \in \mathbb{Z}\}$ and $0 \leq \theta \leq 2\pi$. Since two electrons can occupy each orbital, the degeneracy for $\{|m| \mid m \in \{0, \pm1, \pm2, \ldots\}\}$ is $2, 4, 4, \ldots$, from which the Hückel rule follows: $4 \sum_{i=1} m_i + 2 = 4n + 2$.

The π-orbitals thus have a shell-like structure. As each orbital can occupy two electrons it takes precisely $(4n + 2)$ electrons to fill a shell. In the case of benzene, which is the prime example of an aromatic molecule, there are 6 π-electrons filling up the three lowest molecular orbitals. All of these orbitals are bonding, whereas the three unoccupied orbitals are anti-bonding, explaining much of the great stability of benzene.

5.1 Ring currents

The shell structure of aromatic molecules also has a profound effect on the magnetic properties of these systems. Aromatic molecules are known to exhibit an exalted diamagnetic response to external magnetic fields. When an aromatic molecule is subjected to an external magnetic field perpendicular to the molecular plane, the induced current can flow not only in the individual chemical bonds but also around the conjugated π-system, giving rise to a non-vanishing net current. This ring current is directed so that the secondary induced magnetic field from the current is directed opposite to the external field, as seen in Fig. 5.2. From this figure it can be seen that the net magnetic field is decreased on the inside of the ring and enhanced on the outside of the

(a)   (b)
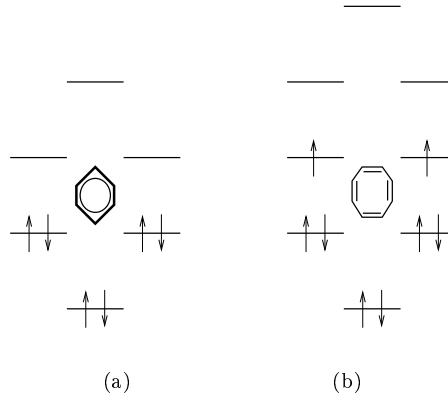
Figure 5.1: Molecular orbital diagrams for the π-electron system in (a) benzene and (b) in cyclotetraoctene.

ring. This effect is sometimes visible in NMR experiments [16, 108], where the outer protons are deshielded compared to normal values for aliphatic molecules. A nucleus on the inside of the ring would experience a stronger magnetic shielding.

5.1.1 Orbital contributions to the ring current

The diamagnetic ring-current effect has been neatly explained in terms of symmetry by Steiner and Fowler [109, 110], and we shall follow their arguments here. For simplicity we shall only consider electrons in an independent-particle model for which the eigenvectors are the MOs and eigenvalues are the orbital energies. Using perturbation theory, the first-order change to an occupied orbital $\psi_n^{(1)}$ can be partitioned into a paramagnetic and a diamagnetic part

$$\psi_n^{(1)} = \psi_n^{(p)} + \psi_n^{(d)} = -\frac{1}{2}\sum_{a>N}\psi_a\frac{\langle\psi_a|\hat{l}|\psi_0\rangle}{\epsilon_a-\epsilon_n}\cdot\mathbf{B} + \frac{1}{2}\mathbf{d}\times\sum_{a>N}\psi_a\frac{\langle\psi_a|\hat{p}|\psi_0\rangle}{\epsilon_a-\epsilon_n}\cdot\mathbf{B}, \qquad (5.1)$$

where the summation runs over all virtual orbitals. When this equation is used in conjunction with Eq. 4.8, it can be shown that $\psi_n^{(p)}$ gives rise to the paramagnetic contribution to the current and $\psi_n^{(d)}$ gives rise to the diamagnetic current. From Eq. 5.1 it is immediately clear that the largest contributions to the perturbed wave function come from the low-lying unoccupied orbitals. Furthermore, the amplitudes are affected by the symmetry of the orbitals and operators. The angular momentum operator $\hat{l}$ spans the irreducible representations (irrep), Γ, for rotational symmetry,
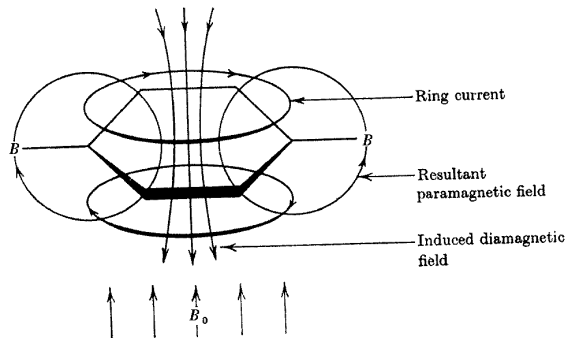
Figure 5.2: Schematic picture of the induced ring current in benzene.

R, of the molecular point group, and the linear momentum operator, $\hat{p}$, spans the translational symmetry T. When the magnetic field is perpendicular to the molecular plane, only $R_{\parallel}$ and $T_{\perp}$ need to be considered as the other components are trivially zero. Thus, the only amplitudes which are non-zero, are those for which

$$A_1 \in \Gamma = \{\Gamma_{\psi_a} \otimes \Gamma_{\{\hat{l},\hat{p}\}} \otimes \Gamma_{\psi_0}\}, \tag{5.2}$$

where A_1 is the totally symmetric irreducible representation. In other words, if the direct product of the orbitals and the operator does not span the totally symmetric component, the integral vanishes. In aromatic molecules, the first accessible transition is to the lowest unoccupied molecular orbital (LUMO) via a translational excitation, giving rise to a large contribution to the diamagnetic response (diatropic current).

In contrast, molecules with a conjugated π-system containing $4n$ electrons behave completely differently. In such systems the largest contributions to the current come, not from the translational transitions, but from rotational excitations making the overall current paratropic. In these molecules, there are usually substantial contributions from translational transitions making the paramagnetic response less pronounced. Molecules sustaining paratropic currents are usually classified as antiaromatic. Antiaromatic molecules are much less common than aromatic molecules. Examples of antiaromatic molecules are cyclotetraoctene (see Fig. 5.1) and cyclodecatrienetriyne, which is discussed more in detail in Article V.

These arguments are of course simplifications, based on some simple Hückel-type Hamiltonian, but the general ideas are valid. In Chap. 6 a method of calculating the current for the full quantum mechanical system is derived. Before doing so we shall look at some qualitative methods to estimate the ring current.

5.2 Types of aromaticity

As pointed out earlier, aromaticity is an elusive phenomenon. As a result, in the pursuit to classify, quantify and understand the subject, aromaticity has been given many subclasses. The following section presents the most common types of aromaticity, with the emphasis on the ring currents. Henceforth, I shall use the word aromaticity as a synonym for ability to sustain a ring current.

5.2.1 Normal aromaticity

Benzene is the epitome of aromaticity. Not only was it the first aromatic molecule to be discovered [111], but it has almost every conceivable characteristic of aromaticity. Benzene has unusually high stability, low reactivity, no bond length alternation in the carbon framework, high magnetic susceptibility, highly deshielded proton shifts corresponding to a strong ring current [1, 69, 112]. The induced current in benzene is visualized in Fig. 5.3. Figure 5.3(a) shows the current in the molecular plane containing the nuclei. By inspection it is easy to see that the net current is nearly zero due to cancellation, and that most of the currents are localized in the σ-bonds. On the other hand, Fig. 5.3(b) shows the current in a plane approximately 0.5 Å above the molecular plane, in the region of large π-electron density, where the ring-current effect is very clearly visible.

In more complicated aromatic molecules, consisting of one or more fused rings, questions arise, not only regarding the ring current, but also about the aromatic pathway. In simple fused molecules like naphthalene the question is easy to answer, but in more complicated systems like porphyrins or coronenes the answer needs a careful analysis [2, 3, 7]. It is interesting to note that the classical law of Kirchoff [113] also holds in molecular systems. The need to understand the aromatic pathways in molecules is not only of academic interest, but can also be of importance to, for example, molecular transistors.

5.2.2 Antiaromaticity

Molecules classified as antiaromatic have $4n$ π-electrons, and thus show a paramagnetic response to magnetic fields. Antiaromatic molecules are not very common, as $4n$ π-electrons usually constitute
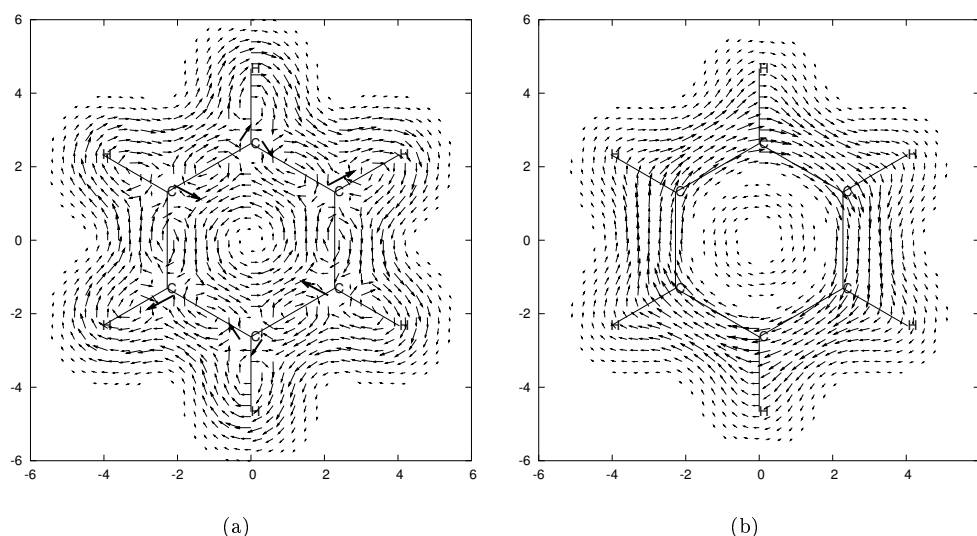
Figure 5.3: Induced current density in benzene calculated at the HF-SCF/TZP level. Figure (a) shows the current density in the plane defined by the nuclei, and Figure (b) shows it 1 Bohr above the molecular plane. The magnetic field is directed perpendicular to the molecular plane.

an open π-shell. Prime examples of a closed-shell antiaromatic molecules are cyclobutadiene and cyclodecatrienetriyne [5, 114].

5.2.3 σ-aromaticity

Ring currents are not only confined to π-electrons as in organic molecules. Certain inorganic molecules can sustain ring currents also in the σ-framework. This phenomenon is probably due to low-lying σ^* and π^* orbitals in metallic rings. An example of a σ-aromatic molecule is Al_4^{2-} [13, 115] which has been observed experimentally.

5.2.4 Homoaromaticity

Homoaromatic molecules are classified as compounds that show aromatic character even though the molecular conjugation is interrupted by single bonds [116, 117, 118]. The concept of homoaromaticity was introduced more than 40 years ago and is still of interest [118]. A family of potentially homoaromatic molecules can be derived from cyclic and conjugated $(4n + 2)\pi$-electron hydrocarbon species by inserting a CH_2 unit into the molecular ring. The best-known example of this kind of species is probably the homotropylium cation $(C_8H_9^+)$ which can be considered as an aromatic $C_7H_7^+$ ion with an additional CH_2 unit. An interesting feature of homo-aromatic aromatic molecules is that the ring current does not follow the molecular framework, but can "leap" through space at the junction of the CH_2 group [6, 116, 117, 118], illustrated schematically for the homotropylium cation in Fig. 5.4.

5.2.5 Spherical aromaticity

A very interesting group of systems are cage molecules of high symmetry. Hirsch [119] initially proposed a revised aromaticity rule for molecules of icosahedral symmetry, in particular fullerenes [120]. In contrast to the normal Hückel $(4n + 2)$ rule for planar systems, molecules of I_h symmetry show complete filling of the electronic shell for $2(n + 1)^2$ π-electrons. This rule has been verified [19, 121, 122] for molecules like, C_{20}^{2+}, C_{60}^{10+} and C_{80}^{8+}. The rule for spherical aromaticity has

later been extended to include other highly symmetrical molecules belonging to the T_d and O_h symmetry point groups [120, 123, 124]. The induced current of C_{60} and C_{60}^{10+} are shown in Fig. 5.5.

Another interesting property of these molecules, both spherical aromatic or not, is to act as magnetic Faraday cages in the sense that the shielding is constant within the shell [69, 125, 126, 127].

5.2.6 Möbius aromaticity

As a curiosity, Heilbronner [128] predicted that singlet $[4n]$annulenes could be aromatic in certain twisted conformations. If the carbon p-orbitals lie on a Möbius-like surface, the annulene should be able to sustain a diatropic current. Schleyer et al. have studied a number of such Möbius annulenes and found them to be aromatic according to the NICS aromaticity index [129] (*vide infra*).

5.3 Nucleus-independent chemical shifts

A very simple method of estimating the aromaticity through the strength of the ring current was proposed by Schleyer *et al.*[17, 18] . The method lends its idea from the aromatic shift observed in ^{1}H NMR experiments and calculations [16]. However, the aromatic contribution to the proton shielding is often relatively small and the proton shieldings also depend significantly on other factors, such as the size of the current circuit, the number of electrons, and the substituents. Thus, the indirect measurement of the strength of the ring current by detecting the proton shieldings does not provide a general method for determining the degree of aromaticity.

Instead of using protons, which have fixed positions in molecules, one calculates the NMR shielding for a "ghost" nucleus which carries no charge, and no basis functions. Such a ghost atom has no effect on the electronic structure of the molecule and can be placed anywhere in the molecule to probe the magnetic shielding. This approach is called the Nucleus-Independent Chemical Shift (NICS) method, and has in recent times become a very popular tool of assessing molecular aromaticity.

In the original proposal [17] one calculates the shielding tensor for one ghost atom located at the center of the molecular ring. For topological reasons the magnetic exaltation is largest near the center of the ring (see Fig. 5.2). Judging from the NICS value one should in principle be able to estimate the strength of the current, and say whether a molecule is aromatic or not.

There are a number of problems with the NICS approach [5, 6, 130]. The first problem is the lack of a reference. Since one cannot simply turn off the current to get a non-aromatic NICS reference value, one must either rely on NICS values for other molecules, or chemical intuition. Neither approach is very satisfactory in terms of reliability. In general, the NICS values are not transferable from one group of molecules to another [19]. They can be used as a relative measure of the aromaticity for closely related molecules, but the NICS values do not provide any accurate information about the strength of the ring current, since the shielding at the center of the molecule depends on both the size of the circuit and the current strength. The second problem is that there is usually substantial electron density at the NICS point, which affects the shielding through both electrostatic and quantum effects. Some of these problems have been acknowledged, and contemporary NICS calculations are often carried out using two NICS values. The NICS(0)
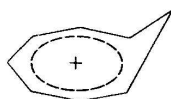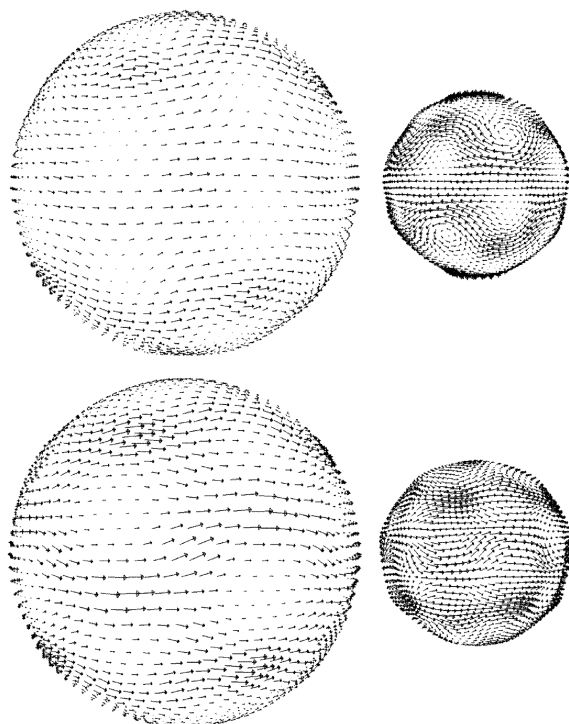

**Figure 5.4:** Schematic illustration of the ring current in the homotropylium cation.

Figure 5.5: The induced currents in neutral (top), and +10 charged (below) fullerene, 1 Å above (right) and below (left) the surface. The magnetic field is directed along the figure plane, from top to bottom.

is calculated in the original NICS point, and an additional NICS(1) is calculated 1 atomic unit (0.52 Å) above the plane. Certain molecules, *e.g.* Al_4^{2-}[13], have diamagnetic short-range shielding, but overall paramagnetic long-range shielding. For such molecules both NICS(0), and NICS(1) values still give faulty answers regarding the aromaticity.

Recently the NICS method has been used to analyze the the so-called anisotropy effect on fragments in NMR experiments [131, 132, 133]. Larger molecules can be considered to be built from a number of functional groups. The shieldings in functional groups can be strongly affected by other groups near-by, causing difficulties in resolving NMR spectra correctly. Functional groups containing double- or triple bonds and, in particular, aromatic rings give rise to highly anisotropic shieldings. In the method of Klod and Kleinpeter [131], NICS values are calculated on a three dimensional grid. By visualizing the isotropic shieldings on isosurfaces the long-range shielding effects of functional groups can be better understood. Using this method they have been able to resolve the NMR spectra for a number of stereo-isomers.

5.4   Aromatic ring-current shieldings

To overcome some of the problems with the NICS approach, we devised a new method, called the Aromatic Ring-Current Shieldings (ARCS) method, in Article I. Instead of probing only *one* point in space, a *set* of points along a line perpendicular to the aromatic ring are probed (see Fig. 5.6). Calculating the nuclear magnetic shielding along this line gives the shielding as a function of distance from the center of the molecule, $\sigma(r)$. As discussed in section 5.1, a ring current circulating in a molecule gives rise to a strong magnetic field which affects the long-range shielding of the probes. Making the assumptions that the current is of a classical nature and that the current loop is circular and infinitely thin, the long-range shielding can be analyzed in terms
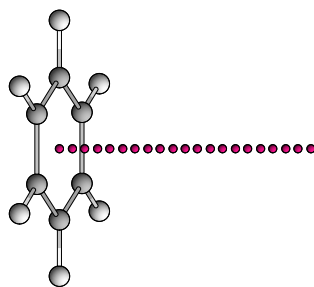
Figure 5.6: A set of ARCS probes in the center of, and perpendicular to, the molecular plane in benzene. Using a single point in the molecular plane would correspond to the NICS(0) index.

of classical electrodynamics. Strictly speaking, the last two assumptions are not necessary but simplify the treatment considerably. Using the Biot-Savart law [134], the long-range shielding can be related back to the strength of the current circulating in the molecule.

The Biot-Savart expression for the magnetic field strength ($\mathbf{B}$) in the vicinity of a thin wire carrying a current I is

$$\mathbf{B} = \frac{\mu_0\, I}{4\pi} \int \frac{d\mathbf{l} \times \mathbf{r}}{r^3}, \tag{5.3}$$

where μ_0 is the permeability of vacuum, $d\mathbf{l}$ is a small length element of the conductor, r is the distance from the wire, and $\mathbf{r}$ is the radial vector from $d\mathbf{l}$ to the probe. Assuming an infinitely thin circular wire, the primitive function of Eq. 5.3 along the symmetry axis of the loop becomes

$$B(z) = \frac{\mu_0\, I}{2} \frac{R^2}{(r^2 + R^2)^{3/2}} = -\sigma(r)B_{ex}, \tag{5.4}$$

where R is the radius of the current loop, r is taken to be the perpendicular distance from the loop center. For large r-values, Eq. 5.4 yields the correct asymptotic behavior of r^{-3} as expected for a magnetic dipole. If the assumptions about the current loop hold, the induced magnetic field is related linearly to the isotropic nuclear magnetic shielding function along the r-axis, $\sigma(r)$, for a given external magnetic field B_{ex}.

Differentiating Eq. 5.4 with respect to the external magnetic field, yields the relation between the isotropic nuclear magnetic shielding and the derivative of the induced current with respect to the applied magnetic field:

$$\sigma(r) = -\frac{\mu_0}{2} \frac{\partial I}{\partial B_{ex}} \frac{R^2}{(r^2 + R^2)^{3/2}}. \tag{5.5}$$

The strength of the induced ring current for a given magnetic field can be obtained as:

$$I = \frac{\partial I}{\partial B_{ex}} B_{ex}. \tag{5.6}$$

Calculating $\sigma(r)$ for a number of r-values in the range $r = [0, r_{max}]$, the induced current derivative ($\frac{\partial I}{\partial B_{ex}}$) and the loop radius ($R$) can be deduced from the long-range part of the shielding function by fitting to Eq. 5.5. Typical values for r_{max} are 30-60 Bohr, depending on the loop size. For small values of r, the shieldings do not obey the Biot-Savarts law for the circular model, as electrostatic and quantum effects of the electron density start to play a role. Also, at short distances, the approximation that the current loop is infinitely thin, is not very good. In order to get reasonable and stable fits it is necessary to use a cut-off, r_{min}, for the shielding function close to the ring. The results are not very sensitive to the choice of r_{min} as long as it is outside the electron charge distribution. Typical r_{min} values are about 3-5 Bohr (1.50-2.50 Å). In many respects the ARCS method can be viewed as an experimental procedure in a theoretical framework.

The degree of aromaticity is usually assumed to be proportional to the strength of the induced ring current which is a measure of the delocalization of the π-electrons [15]. The degree
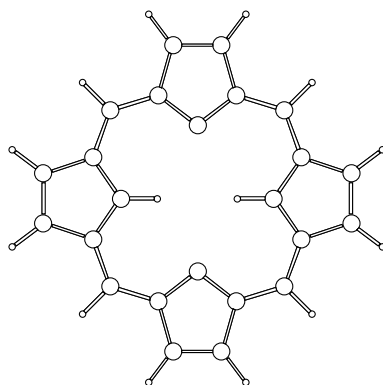
Figure 5.7: The molecular structure of free-base porphyrin.

of aromaticity of any molecule, deduced from the calculated ARCS data, can then be compared regardless of the size of the aromatic path. More precisely, the shieldings are proportional to the derivative of the current strength with respect to the applied magnetic field, while the ring current depends on the field strength. Figure 5.8 shows the result of an ARCS calculation for free-base porphyrin.

While the ARCS method has proved to be a very useful tool to calculate the over-all strength of the ring current in molecules, it cannot convey any details about the structure of the currents in molecules. The need to obtain more detailed information about the currents becomes evident for more complicated molecules consisting of multiple or fused aromatic rings. For example free-base porphyrin (see Fig. 5.7) consists of four pyrrole groups connected by conjugated bonds to form a macro cycle, and has ring currents which are rich in detail (see Articles II, III and VII in the Appendix). In an attempt to analyze this underlying structure we developed a method called Planar ARCS (PARCS).

In the PARCS approach, the shielding function is calculated in a plane parallel to the molecular plane at a distance from it. The PARCS data provides some information about anisotropies in the ring currents, but it does not directly yield any information about the fine structure of the currents. It is, however, possible to manipulate the PARCS data in order to get more detailed information about current paths. The calculated two-dimensional PARCS functions can be expanded in two-dimensional momentum functions analogously to the expansion in spherical harmonics in the three-dimensional case

$$\phi(x,y) = \sum_i f_i(r)\chi_i(\theta), \tag{5.7}$$

where $\chi_i(\theta)$ are angular functions *i.e.* s, p_x, p_y, $d_{x^2-y^2}$, and d_{xy}, while $f_i(r)$ are the corresponding radial parts. The radial functions for the first few angular functions can be obtained by numerical integration and Gram-Schmidt orthogonalization. The projected PARCS functions are obtained as

$$\tilde{\varphi}(r,\theta) = \varphi(r,\theta) - \sum_k \frac{\int \chi_k(\theta)\varphi(r,\theta)d\theta}{\int \chi_k^2(\theta)d\theta}\chi_k(\theta) \ . \tag{5.8}$$

By projecting out the dominating s-term and eventually some of the higher-order terms from the two-dimensional PARCS function, the underlying fine structure of the ring current is revealed. The results of the PARCS analysis for free-base porphyrin are shown in Fig. 5.9. Figure (b) clearly shows the existence of stronger local currents in the pyrrole units with an inner hydrogen.

(a)   (b)
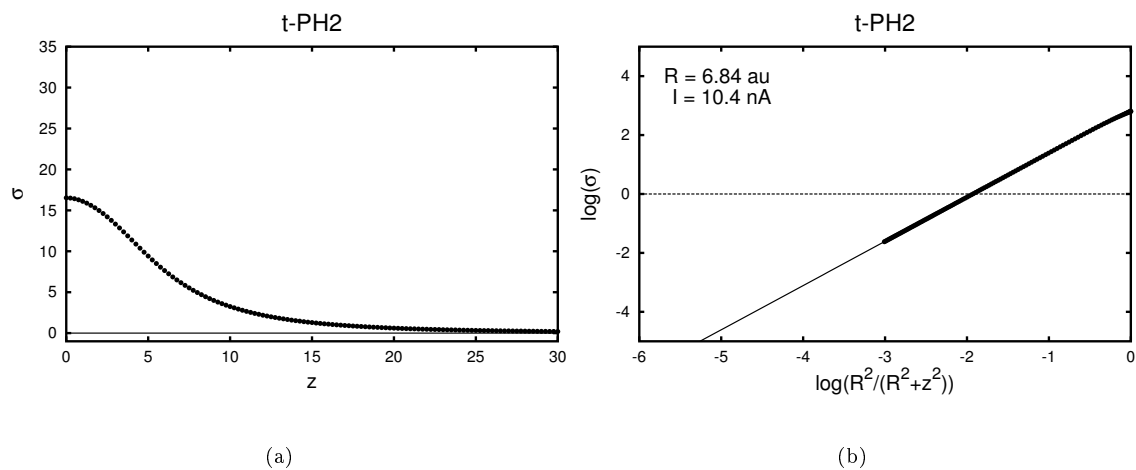
Figure 5.8: The calculated ARCS functions (a) for free-base porphyrin (in ppm) and (b) the logarithmic fit of the ARCS functions to Eq. (5.5).

(a)   (b)
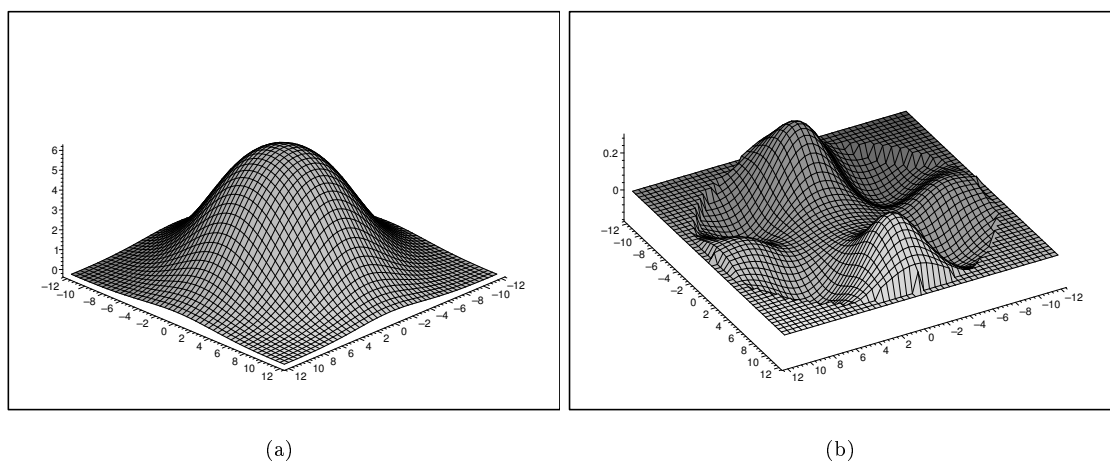
Figure 5.9: (a) The nuclear magnetic shieldings for free-base porphin calculated at a distance of 7 Bohr from the molecular plane. (b) The PARCS function after the circular symmetric part has been projected out.

Chapter 6

Calculation of magnetically induced currents

We shall now turn from qualitative ring-current models to methods for explicitly treating the magnetically-induced quantum-mechanical current density. The methods presented here are concerned with the time-independent current density in closed-shell molecules.

The first calculations of ring currents were based on simple model Hamiltonians of Hückel type. Some of the earliest work goes back to Pauling, London and Lonsdale [78, 135, 136]. Pople later refined and extended their ring-current model, in an attempt to explain the proton NMR shifts in aromatic molecules [137]. Even though the use of GIAOs is currently the most popular approach of resolving the gauge-origin issue in shielding calculations [138], magnetically induced current densities have in most cases been obtained using computational methods with an explicit gauge-origin dependence. One such method is the the Continuous Transformation of the Origin of the Current Density (CTOCD) method [69, 139, 140, 141] which has been widely used to visualize the magnetically induced current density and current in molecules.

The Gauge-Including Magnetically Induced Currents method (GIMIC) is a new method of calculating the current density in molecules. The GIMIC method is formulated in the framework of derivative theory, and relies on the use of GIAOs for rapid basis-set convergence and gauge independence. Since the theory is derived in terms of density matrices, it is applicable also in conjunction with correlated wave functions such as Møller–Plesset, coupled-cluster and multiconfigurational (MCSCF) wave functions.

6.1 Continuous transformation of the origin of the current density

The partitioning of the current density into paramagnetic and diamagnetic contributions in Eq. 4.8 is somewhat arbitrary, as the terms are dependent on the chosen gauge origin of the external magnetic field. This property of the current density was first used by Hirschfelder and Heller [142] to annihilate the paramagnetic terms to the one-electron current density using gauge transformations. Their derivation was based on a hydrodynamical formulation of quantum mechanics. Later Keith and Bader [95, 139, 140] showed that also the N-electron diamagnetic current-density term can be formally annihilated at every point in space using a "continuous set of gauge transformations". A gauge transformation which shifts the gauge by a vector $\mathbf{d}$, $\mathbf{r}_O \rightarrow \mathbf{r}' = \mathbf{r}_O + \mathbf{d}$, leaves the total current density in any point, $\mathbf{r}$, invariant

$$\mathbf{J^B}(\mathbf{r} - \mathbf{r}') = \mathbf{J}_d^{\mathbf{B}}(\mathbf{r} - \mathbf{r_O}) + \mathbf{J}_d^{(\mathbf{r}'-\mathbf{r_O})\times\mathbf{B}}(\mathbf{r}) + \mathbf{J}_p^{\mathbf{B}}(\mathbf{r} - \mathbf{r_O}) + \mathbf{J}_p^{(\mathbf{r}'-\mathbf{r_O})\times\mathbf{B}}(\mathbf{r}) = \mathbf{J^B}(\mathbf{r} - \mathbf{r_O}). \quad (6.1)$$

By choosing the gauge origin to coincide with the point of interest, $\mathbf{r}' = \mathbf{r}$, the diamagnetic terms are annihilated since

$$\mathbf{J}_{\mathrm{d}}^{\mathbf{B}}(\mathbf{r} - \mathbf{r_O}) = -\mathbf{J}_{\mathrm{d}}^{(\mathbf{r}-\mathbf{r_O})\times\mathbf{B}}(\mathbf{r}). \tag{6.2}$$

As such, this approach is not very useful since it implies that the perturbed wave function must be calculated separately for every point where the current density is calculated.

Lazzeretti *et al.* [143] showed that it is beneficial to view the gauge transformation in terms of a displacement function $\mathbf{d}(\mathbf{r}) = \mathbf{r}$, instead of a constant displacement $\mathbf{d}$. It's then possible to show that the point-wise procedure of Keith and Bader is not necessary, and that the problem can be given a fully analytical solution. This is the basis for the Continuous Transformation of the Origin of the Current Density (CTOCD) methods [28, 69, 141, 143, 144, 145, 146, 147, 148]. When the diamagnetic term is quenched the method gets the acronym CTOCD-DZ [143, 144], where DZ stands for Diamagnetic Zero. In a similar manner it is also possible to annihilate the paramagnetic terms, giving the CTOCD-PZ (Paramagnetic Zero) method [145, 146, 147, 149].

6.2 The GIMIC method

Here we present a new computational approach to calculate magnetically induced current densities, based analytical derivative theory in conjunction with GIAOs. The derivation is based on the Biot-Savart expression for the nuclear magnetic shielding tensor [69, 143, 150] as well as the corresponding expressions obtained within analytic derivative theory [62, 86, 92, 99, 101, 104]. By combining these expressions, the resulting equations only require knowledge about the basis set as well as the unperturbed and perturbed one-electron density matrices. Using this approach, current densities can be calculated at all computational levels for which the relaxed one-electron density matrices are available. Due to the use of GIAOs, no reference to the gauge origin appears in the final expression for the first-order induced current density. The obtained currents are gauge-origin independent but gauge invariance is achieved only in the limit of a complete basis set. GIAOs have previously been used in a similar approach, to calculate current densities in conjunction with magnetizabilities [151].

6.2.1 Analytic derivative-based current-density theory

To derive a set of equations for the current density in conjunction with GIAOs, we start from two different energy expressions. The general energy expression in Eq. 2.12 needs formally no modification itself in order to account for an external magnetic field or the GIAOs

$$E = \sum_{\mu\nu} h_{\mu\nu} D_{\mu\nu} + \frac{1}{2} \sum_{\mu\nu\sigma\rho} g_{\mu\sigma\nu\rho} d_{\mu\sigma\nu\rho}. \tag{6.3}$$

All modifications to Eq. 6.3, go into the density matrices, and the one-electron operator $\hat{h}$, which affects the densities through the integrals. In the presence of an external magnetic field the kinetic energy operator is replaced by the canonical momentum operator

$$\boldsymbol{\pi}\cdot\boldsymbol{\pi} = \mathbf{p^2} + 2\mathbf{A^B}\cdot\mathbf{p} + 2\mathbf{A^{m_I}}\cdot\mathbf{p} + 2\mathbf{A^B}\cdot\mathbf{A^{m_I}} + \mathbf{A^B}\cdot\mathbf{A^B} + \mathbf{A^{m_I}}\cdot\mathbf{A^{m_I}}, \tag{6.4}$$

where $\mathbf{A} = \mathbf{A^m} + \mathbf{A^B}$ is the vector potential for the external and internal magnetic fields defined in Eq. 4.6 and Eq. 4.7.

The nuclear magnetic shielding is given as the second-order change of the energy with respect to the nuclear magnetic moments and the external magnetic field

$$\sigma_{\alpha\beta}^{I} = \left.\frac{\partial^2 E}{\partial m_{\alpha}^{I} \partial B_{\beta}}\right|_{\substack{\mathbf{B=0} \\ \mathbf{m}_I=0}}. \tag{6.5}$$

Differentiating the total energy in Eq. (6.3) with respect to the nuclear magnetic moments and the components of the external magnetic field, in the limit of zero magnetic field, yields

$$\sigma_{\alpha\beta}^I = \sum_{\mu\nu} D_{\mu\nu} \frac{\partial^2 h_{\mu\nu}}{\partial m_\alpha^I \partial B_\beta} + \sum_{\mu\nu} \frac{\partial D_{\mu\nu}}{\partial B_\beta} \frac{\partial h_{\mu\nu}}{\partial m_\alpha^I}, \tag{6.6}$$

where $\partial D_{\mu\nu}/\partial B_\beta$ are the perturbed density matrices, and $\partial h_{\mu\nu}/\partial m_\alpha^I$ and $\partial^2 h_{\mu\nu}/\partial m_\alpha^I \partial B_\beta$ are the corresponding derivatives of the integrals of $\hat{h}$ in the AO representation.

The second energy expression we need is the Biot-Savart expression for the magnetic interaction energy in terms of the induced current and the magnetic vector potential [69]

$$E^{mB} = -\frac{1}{c} \int \mathbf{A}^{m_I}(\mathbf{r}) \cdot \mathbf{J}^{\mathbf{B}}(\mathbf{r}) d\mathbf{r}. \tag{6.7}$$

Evaluating the second derivative in Eq. (6.5) for the Biot-Savart energy in Eq. (6.7) yields

$$\sigma_{\alpha\beta}^I = -\sum_\gamma \epsilon_{\alpha\delta\gamma} \int \frac{r_\delta - R_{I\delta}}{|\mathbf{r} - \mathbf{R}_I|^3} \mathcal{J}_\gamma^{B_\beta} d\mathbf{r}, \tag{6.8}$$

where

$$\mathcal{J}_\gamma^{B_\beta}(\mathbf{r}) = \frac{\partial J_\gamma(\mathbf{r})}{\partial B_\beta}, \tag{6.9}$$

are the tensor elements of the first-order induced current density, and $\epsilon_{\alpha\delta\gamma}$ is the Levi-Civita tensor*.

The two equations for the nuclear magnetic shielding tensor now allow us to make a connection between the expression containing the current-density tensor and the second-derivative expression for σ. Equating Eq. 6.6 and Eq. 6.8 and explicitly introducing the one-electron basis functions, we obtain the following equation that relates nuclear magnetic shieldings and the current-density tensor

$$\int \sum_{\mu\nu} D_{\mu\nu} \frac{\partial^2}{\partial m_\alpha^I \partial B_\beta} \left\{ \chi_\mu^*(\mathbf{r}) \hat{h} \chi_\nu(\mathbf{r}) \right\} d\mathbf{r} + \int \sum_{\mu\nu} \frac{\partial D_{\mu\nu}}{\partial B_\beta} \frac{\partial}{\partial m_\alpha^I} \left\{ \chi_\mu^*(\mathbf{r}) \hat{h} \chi_\nu(\mathbf{r}) \right\} d\mathbf{r}$$
$$= -\sum_\gamma \epsilon_{\alpha\delta\gamma} \int \frac{(r_\delta - R_{I\delta})}{|\mathbf{r} - \mathbf{R}_I|^3} \mathcal{J}_\gamma^{B_\beta}(\mathbf{r}) d\mathbf{r}. \tag{6.10}$$

Since Eq. 6.6 is implicitly dependent on the current density through Eq. 4.12, the left- and right-hand side integrands in Eq. 6.10 must be equal, defining the current-density tensor in a point in space. Together with the use of field-dependent basis functions (Eq. 4.26), we get the following relation for the tensor

$$-\epsilon_{\alpha\delta\gamma} \frac{(r_\delta' - R_{I\delta})}{|\mathbf{r}' - \mathbf{R}_I|^3} \mathcal{J}_\gamma^{B_\beta}(\mathbf{r}')$$
$$= \sum_{\mu\nu} D_{\mu\nu} \chi_\mu^*(\mathbf{r}') \frac{\partial^2 \hat{h}}{\partial m_\alpha^I \partial B_\beta} \chi_\nu(\mathbf{r}') + \sum_{\mu\nu} \frac{\partial D_{\mu\nu}}{\partial B_\beta} \chi_\mu^*(\mathbf{r}') \frac{\partial \hat{h}}{\partial m_\alpha^I} \chi_\nu(\mathbf{r}')$$
$$+ \sum_{\mu\nu} D_{\mu\nu} \frac{\partial \chi_\mu^*(\mathbf{r}')}{\partial B_\beta} \frac{\partial \hat{h}}{\partial m_\alpha^I} \chi_\nu(\mathbf{r}') + \sum_{\mu\nu} D_{\mu\nu} \chi_\mu^*(\mathbf{r}') \frac{\partial \hat{h}}{\partial m_\alpha^I} \frac{\partial \chi_\nu(\mathbf{r}')}{\partial B_\beta}, \tag{6.11}$$

where the last two terms arise due to the GIAOs. The derivatives of the one-electron Hamiltonian are

$$\left. \frac{\partial \hat{h}}{\partial \mathbf{m}_I} \right|_{\substack{\mathbf{B}=\mathbf{0} \\ \mathbf{m}_I=\mathbf{0}}} = -\frac{i}{c} \frac{(\mathbf{r} - \mathbf{R}_I) \times \nabla}{|\mathbf{r} - \mathbf{R}_I|^3} \tag{6.12}$$

---

*$\epsilon_{\alpha\sigma\gamma} = 1$ for even permutations of the indices, $\epsilon_{\alpha\sigma\gamma} = -1$ for odd permutations. When any two indices coincide, $\epsilon_{\alpha\sigma\gamma} = 0$.

$$\frac{\partial^2 \hat{h}}{\partial \mathbf{m}_I \partial \mathbf{B}}\bigg|_{\substack{\mathbf{B}=0 \\ \mathbf{m}_I=0}} = \frac{1}{2c^2} \frac{(\mathbf{r}-\mathbf{R}_O)\cdot(\mathbf{r}-\mathbf{R}_I)\mathbf{1}-(\mathbf{r}-\mathbf{R}_O)(\mathbf{r}-\mathbf{R}_I)}{|\mathbf{r}-\mathbf{R}_I|^3}. \tag{6.13}$$

Equation 6.11 can be further simplified by noting that the denominators $|\mathbf{r}-\mathbf{R}_I|^3$ cancel. Defining a new set of operators, $\partial \tilde{h}/\partial m_\alpha^I$ and $\partial^2 \tilde{h}/\partial m_\alpha^I \partial B_\delta$, without the denominator $|\mathbf{r}-\mathbf{R}_I|^3$, the components of the magnetically induced current-density tensor, $\mathcal{J}_\alpha^{B_\beta}(\mathbf{r})$ can be obtained as

$$\mathcal{J}_\alpha^{B_\beta}(\mathbf{r}') = -\epsilon_{\alpha\beta\delta}\sum_{\mu\nu} D_{\mu\nu}\chi_\mu^*(\mathbf{r}')\frac{\partial^2 \tilde{h}}{\partial m_\alpha^I \partial B_\delta}\chi_\nu(\mathbf{r}') + \sum_{\mu\nu}\frac{\partial D_{\mu\nu}}{\partial B_\beta}\chi_\mu^*(\mathbf{r}')\frac{\partial \tilde{h}}{\partial m_\alpha^I}\chi_\nu(\mathbf{r}')$$

$$+ \sum_{\mu\nu} D_{\mu\nu}\frac{\partial \chi_\mu^*(\mathbf{r}')}{\partial B_\beta}\frac{\partial \tilde{h}}{\partial m_\alpha^I}\chi_\nu(\mathbf{r}') + \sum_{\mu\nu} D_{\mu\nu}\chi_\mu^*(\mathbf{r}')\frac{\partial \tilde{h}}{\partial m_\alpha^I}\frac{\partial \chi_\nu(\mathbf{r}')}{\partial B_\beta}. \tag{6.14}$$

Equation 6.14 is easily evaluated at any point in space (except at the nuclei), since it only involves basis functions and derivatives of basis functions at that point as well as the corresponding one-electron density matrices. The unperturbed AO density matrix is obtained by solving some approximate Schrödinger equation, as outlined in Chap. 2. The perturbed AO density matrices are obtained by solving the CPHF equations in Chap. 3.1, at the corresponding level of approximation.

The quantities that need to be evaluated in Eq. 6.14 are

$$\frac{\partial \chi_\mu(\mathbf{r})}{\partial B_\alpha} = -\frac{i}{2c}\sum_\gamma \epsilon_{\alpha\beta\gamma}\tilde{r}_\gamma(R_{\mu\beta}-R_{O\beta})\chi_\mu(\mathbf{r}) \tag{6.15a}$$

$$\frac{\partial \tilde{h}}{\partial m_\alpha^I}\chi_\mu(\mathbf{r}) = \sum_\gamma \epsilon_{\alpha\beta\gamma}\tilde{r}_\gamma\left(l_\beta \tilde{r}_\beta^{-1} - 2\xi\tilde{r}_\beta\right)\chi_\mu(\mathbf{r}) \tag{6.15b}$$

$$\frac{\partial \tilde{h}}{\partial m_\alpha^I}\frac{\partial \chi_\mu(\mathbf{r})}{\partial B_\beta} = \sum_\gamma \epsilon_{\alpha\delta\gamma}\tilde{r}_\gamma\left[(\frac{i}{c}\xi\tilde{r}_\delta - l_\delta\tilde{r}_\delta^{-1})\sum_\eta \epsilon_{\alpha\sigma\eta}r_\sigma'(R_{\mu\eta}-R_{O\eta})\right]\chi_\mu(\mathbf{r})$$

$$+ \sum_\gamma \epsilon_{\alpha\delta\gamma}\tilde{r}_\gamma\left[\epsilon_{\alpha\beta\gamma}\frac{i}{2c}(R_{\mu\gamma}-R_{O\gamma})\right]\chi_\mu(\mathbf{r}) \tag{6.15c}$$
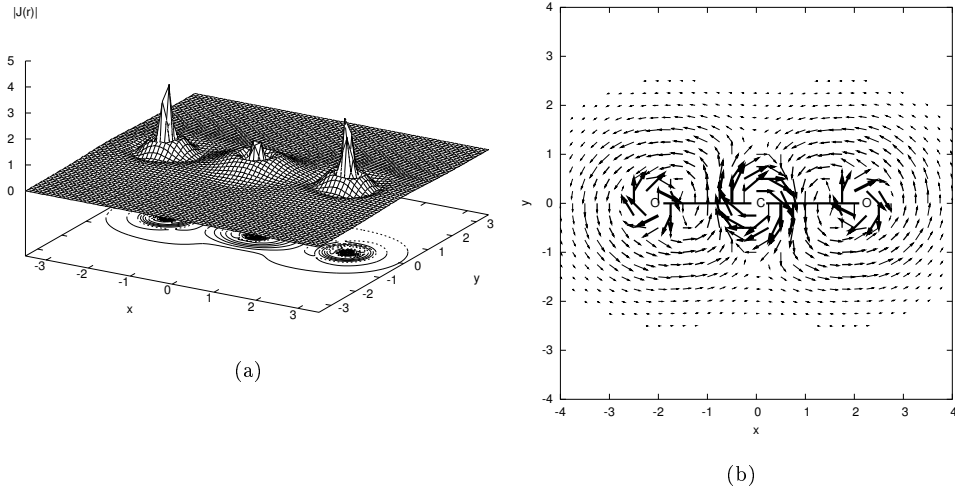
$$\frac{\partial^2 \tilde{h}}{\partial m_\alpha^I \partial B_\beta}\chi_\mu(\mathbf{r}) = \left(\delta_{\alpha\beta}\left[\frac{1}{2c^2}\sum_\delta(r_\delta'-R_{O\delta})\tilde{r}_\delta\right] - (r_\alpha'-R_{O\alpha})\tilde{r}_\beta\right)\chi_\mu(\mathbf{r}). \tag{6.15d}$$

where ξ is an AO exponent. In the above equations $\tilde{r}_\alpha = r_\alpha - R_{\mu\alpha}$, where $R_{\mu\alpha}$ is a component of the μ:th origin of the basis function, R_O refers to to the global gauge origin and r' is an absolute coordinate.

It should be noted that the explicit dependence of each individual contribution on the nuclear position $\mathbf{R}_I$ cancels out in the sum of all contributions, making the expression for the current-density tensor independent of the nuclear positions $\mathbf{R}_I$ and the magnetic moments m_α^I, as it should be. The operator in Eq. 6.13 is still explicitly dependent on the gauge origin $\mathbf{R}_O$, which seems to render the current tensor gauge dependent. It can be shown that the gauge-dependent terms cancel exactly against terms arising from the differentiation of the GIAOs.

Equation 6.14 can be recast in a matrix-vector form to allow for easy implementation in a computer program. Let $\mathbf{v}$ be a vector whose elements consist of the basis-function values at a grid point $\mathbf{r}$. We also need to evaluate the first derivatives of the basis functions with respect to the components of the external magnetic field as well as a mixed second derivative with respect to $\mathbf{B}$ and $x, y,$ and z. The vectorized equivalent of expression Eq. 6.14 for $\mathcal{J}_\alpha^{B_\beta}(\mathbf{r})$ is then given by

$$\mathcal{J}_\alpha^{B_\beta} = -\sum_\gamma \epsilon_{\alpha\beta\gamma}\frac{1}{2}(\mathbf{v^T Dv})\mathbf{r}_\gamma + \mathbf{v^T P}_\beta \mathbf{d}_\alpha - \mathbf{b}_\beta^{\mathbf{T}}\mathbf{Dd}_\alpha + \mathbf{v^T Dq}_{\alpha\beta} \tag{6.16}$$

Figure 6.1: The magnitude (a) and direction (b) of the induced current density (in au) calculated in the molecular plane of CO_2 at the CCSDT/TZP level.

with $\mathbf{D}$ as the AO density matrix, $\mathbf{P}_\alpha$ the perturbed AO density matrices, and the quantities (equivalents of Eq. 6.15a-c) $\mathbf{b}_\alpha, \mathbf{d}_\alpha, \mathbf{q}_{\alpha\beta}$ given by

$$\mathbf{b}_\alpha = \frac{\partial \mathbf{v}}{\partial \mathbf{B}_\alpha} \tag{6.17a}$$

$$\mathbf{d}_\alpha = \frac{\partial \mathbf{v}}{\partial r_\alpha} \qquad (\alpha, \beta = x, y, z) \tag{6.17b}$$

$$\mathbf{q}_{\alpha\beta} = \frac{\partial^2 \mathbf{v}}{\partial \mathbf{r}_\alpha \mathbf{B}_\beta}. \tag{6.17c}$$

The density matrices $\mathbf{D}$ and $\mathbf{P}_\alpha$ are obtained from standard *ab initio* and DFT program packages capable of calculating nuclear magnetic shielding tensors.

Knowledge of the first-order current tensors allows us to calculate the current density by contracting the tensors against a magnetic field, which has both direction and magnitude. Calculating a set of tensors on a suitable grid enables us to make plots of the magnetically induced current density in molecules. Furthermore, in section 6.2.2 we shall show how the absolute strength of the current can be calculated.

The theory outlined above has been implemented in a computer program [7], and subsequently used to calculate induced currents in a number of molecules [10, 12, 13].

6.2.2   Integration of current densities

Although the current density is a proper quantum mechanical observable, it has not been directly observed experimentally. As such, current-density maps can convey new, otherwise inaccessible, information about molecules, thus aiding the understanding of the current paths in the molecule. However, current-density plots do not provide any quantifiable measures of the current strengths nor are they suitable for comparing current strengths in different molecular systems. By integration over the current flow passing through specific bonds, it is possible to obtain the net current strengths around a molecular ring or through a bond. In non-cyclic molecules, the net current flow must be zero, in order for the law of charge conservation to hold.

Integration of the current density is done using two-dimensional Gaussian or Lobatto quadrature [152] over a bond cross section (see Fig. 6.2). The Gauss integration points x_i are given by
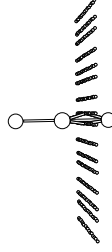
Figure 6.2: A typical integration grid through a bond.

the nodes of the Legendre polynomials $P_n(x)$, while the integration weights w_i^G are obtained from the differentiated polynomials, $\left(\frac{dP_n(x_i)}{dx}\right)$. In one dimension, Gauss quadrature yields

$$\int_a^b f(x)dx = \sum_{k=1}^m \left(\sum_{i=1}^n w_i^G f_k(x_i)\right), \tag{6.18}$$

where the sum over k originates from the piecewise integration and f_k is the function f shifted to $[-1, 1]$ on the kth interval. The integration weights are given by

$$w_i^G = \frac{2}{1 - x_i^2}\left(\frac{dP_n(x_i)}{dx}\right)^2. \tag{6.19}$$

In the Lobatto integration, the integration points are determined via the nodes of the first derivative of the Legendre polynomials of order $n-1$, $\left(\frac{dP_{n-1}(x)}{dx}\right)$. In addition, the function values at the end points of the interval are also considered in the Lobatto integration. The integration weights w_i^L are obtained from $P_{n-1}(x_i)$. The one-dimensional Lobatto quadrature then reads

$$\int_a^b f(x)dx = \sum_{k=1}^m \left(w_1^L f_k(-1) + w_n^L f_k(1) + \sum_{i=2}^{n-1} w_i^L f_k(x_i)\right), \tag{6.20}$$

with the corresponding weights given by

$$w_i^L = \frac{2}{n(n-1)\left(P_{n-1}(x_i)\right)^2}, \tag{6.21}$$

and the integration weights for the end points by

$$w_1^L = w_n^L = \frac{2}{n(n-1)}. \tag{6.22}$$

Numerical values for the integration points and weights are tabulated in Ref. [152]. Alternatively they can be obtained by solving the roots to the derivative of the Legendre polynomials, using for example Newton's method.

Cyclic systems such as aromatic molecules can sustain a net current that flows around the molecular rings. The net current should in principle be independent of where in the ring it is calculated. Due to practical issues, this is not necessarily always the case. In the numerical integration of the currents passing a given bond, one has to be careful where and how to cut the bond. The choice of grid and method of integration is, by far, less critical. For benzene, a fairly good convergence of the integrated current is achieved with a grid that starts in the ring center, passes through the center of the bond, and is perpendicular to the molecular plane. The integration area has to be extended to about 5 Bohr outside the bond and 5 Bohr above and below

the ring. Then, it incorporates the most significant part of the current flow. In principle, it does not matter for which bond cross section the ring current is integrated, but it is recommended to use cross sections containing the bond midpoint. The reason is that due to the poles at the nuclei the current-density vector field can be rather strong in the vicinity, which thus renders integration more difficult. Dense grids are then needed to converge the integrals, while, for integrations over bond cross sections containing the bond midpoint, as few as 20 grid points in each direction are often sufficient for obtaining accurate integral values. The divergence problem discussed in the next subsection also suggests that the integration plane is chosen as far away from the nuclei as possible.

For non-cyclic molecules (e.g. carbon dioxide, ozone) the net current is necessarily zero. In spite of this, it is still possible to obtain the strength of the current in individual bonds by splitting the integral into positive and negative contributions, or alternatively, by integrating over only half of the bond cross section. Currents obtained in such a way are however dependent on the location of the cut-plane. Such "bond currents" might prove useful as a measure of electron delocalization.

6.2.3   Current conservation in the GIMIC method

As mentioned earlier, the current obeys the law of charge conservation, *i.e.* the divergence of the current, $\nabla \cdot \mathbf{J}$, must be zero at *every* point of space*. Alternatively, the law of charge conservation can be expressed using the Sambe-Epstein integral condition for charge-current conservation [69]

$$\int \mathbf{J}(\mathbf{r}) \cdot d\mathbf{r} = 0. \tag{6.23}$$

For molecules with a center of inversion this integral is for symmetry reasons equal to zero, whereas for molecules of low symmetry, Eq. 4.11 is fulfilled only when charge is conserved. Requiring the divergence to be zero is thus a better criterion, as it is a local measure of charge conservation.

The law of charge conservation can also be viewed as a consequence of gauge invariance [70]. Thus, if true gauge invariance is not achieved, the calculated current will to some extent be divergent. Epstein has shown that the use of GIAOs does not necessarily lead to the desired current conservation [70] even though the magnetic shielding tensor is gauge-origin independent. This is not surprising, since the GIAO approach can be viewed as a recipe for the unique definition of a set of local gauge-origins for the basis functions. Gauge-origin dependence is in this way eliminated, but gauge invariance cannot achieved in this manner.
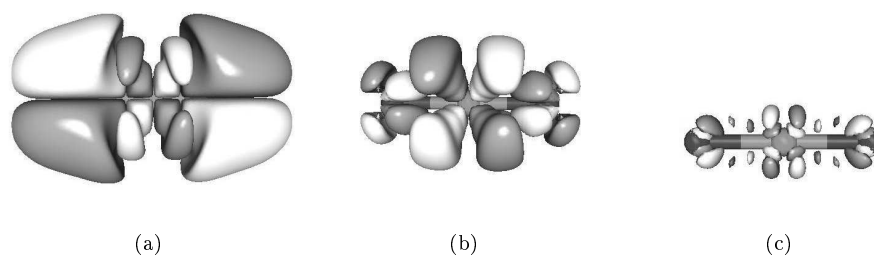
By calculating the divergence of the current ($\nabla \cdot \mathbf{J}(\mathbf{r})$) in selected points of space, one can obtain a measure of the gauge-independence errors, and thus of the basis-set completeness. In our work, the divergence is calculated by using numerical differentiation on a locally tight grid.

Calculations of the divergence for H_2 and CO_2 at the HF-SCF level showed that the divergence of the current significantly deviates from zero in the vicinity of the nuclei, and in regions where the direction of the current changes rapidly. By systematically augmenting the basis sets with functions of higher l-quantum numbers, the divergence converges towards small values even close to the nuclei [see Figure 6.3(b) and (c)]. For H_2, the use of a basis set of cc-pV5Z quality to reduces the maximum value of the divergence to a value which is for all practical purposes equal to zero. The same quality basis for CO_2 still yields non-zero divergence near the nuclei. Discouraging as this may seem, a corresponding HF-SCF/SVP calculation without GIAOs and with the gauge origin at the carbon atom yields a maximum value of the divergence which is more than factor of fifteen times larger than the largest divergence of the GIAO calculation. In the conventional calculation, the divergence also has a much broader spatial distribution. The effect of the GIAOs on the divergence can clearly be seen in Figure 6.3 (a) and (b).

Judging whether a divergence is large or not always easy. Therefore, one has to examine other properties of the current to be able to evaluate the quality of the results. The difference in the currents calculated at the HF-SCF/SVP and HF-SCF/cc-pV5Z levels is found to be small.

---

*This requirement holds for time-independent systems. For time-dependent systems, the divergence must be equal to a corresponding change of the density at time t.

(a)   (b)   (c)

Figure 6.3: The divergence of the current in CO_2 obtained in a conventional HF-SCF/SVP calculation (a). The corresponding divergence plots obtained at the GIAO HF-SCF/SVP and the GIAO HF-SCF/cc-pV5Z levels are depicted in (b) and (c), respectively. The iso-surfaces have been drawn to encompass any divergence larger than 0.01.

By studying the convergence of the integrated current through a bond, one finds that the induced current only changes by few percent when increasing the basis-set size from SVP to cc-pV5Z. At the HF-SCF level, the integrated value for the current passing half of the bond in CO_2 decreases from 10.03 to 9.81 nAT^{-1} when increasing the basis-set size from SVP to cc-pV5Z. For non-cyclic molecules, for which the symmetry does not constrain the total current to be zero, the effects of the non-zero divergence can be seen more clearly. In water and ozone, which belong to the C_{2v} point group, the integrated current through the symmetry plane is particularly hard to converge to zero, because the cut plane goes through a nucleus where the divergence is large. For water, the difference between positive and negative current contributions calculated at the HF-SCF/SVP level is 0.68 nAT^{-1} as compared to the individual contributions of 24.67 nAT^{-1} and -23.99 nAT^{-1}, respectively. The corresponding values obtained in a HF-SCF/cc-pV5Z calculation are 0.0002 nAT^{-1}, 23.4171 nAT^{-1} and -23.4169 nAT^{-1}, respectively. By evaluating the Sambe-Epstein condition in Eq. (4.11) separately for each tensor component, one can estimate the total current leakage. At the HF-SCF/SVP level, the total leakage of the xy and yx components of the current tensor is -3.95 and 2.45 nAT^{-1} for water, respectively, whereas at the HF-SCF/cc-pV5Z level, the corresponding values are -0.2295 nAT^{-1} and 0.0044 nAT^{-1}. Thus, even though the divergence is not equal to zero in every point in space and the current leakage does not seem to be negligible, the integrated currents are pretty well converged even when using fairly small standard basis sets.
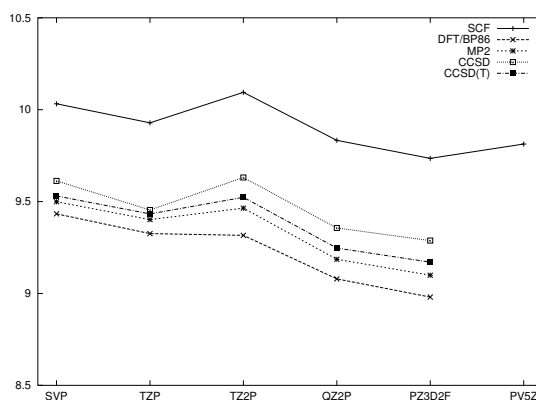
Figure 6.4: The basis-set convergence for the induced current (in nAT^{-1}) calculated at the HF-SCF, DFT-BP86, MP2, CCSD, and CCSD(T) levels for CO_2.

Chapter 7

Summary and outlook

When the work upon which this thesis is based was started, we were interested in the aromaticity and the aromatic pathways of free-base porphyrins. We set out trying to analyze the aromaticity using the, then new, NICS method. Quite soon we found ourselves head deep in data which proved very hard to draw any final conclusions from. Instead of drawing far-fetched conclusions, we started experimenting with the NICS approach, adding NICS points in the direction perpendicular to the molecular plane. This experimenting lead to the ARCS method which is presented in Article I. In this paper we developed the ARCS analysis and applied it to a number of simple aromatic and non-aromatic molecules.

At this stage, we were confident that we had a much more reliable method than the original NICS method. In Article II we returned to the porphyrin problem, and using the ARCS method we analyzed the aromaticity and the current pathways. To resolve the current pathways in these fused-ring systems, we saturated certain bonds, effectively preventing any current to take that route. By calculating the current strengths, we were able to deduce the preferred paths indirectly. In the original ARCS paper, we had also tried to use a 2D-NICS, in which two-dimensional layers of NICS points were calculated at some distance from the molecular plane. This approach, which we called Planar ARCS (PARCS), came in handy for giving additional evidence for our conclusions. It is interesting to note that our conclusions about free-base porphyrin, were later verified using the GIMIC method [7]. In Article III we studied the aromaticity of magnesium porphyrins. In this paper, we asked the question, of the significance of the inner hydrogen pair for the ring current. This paper was in a sense an extension of the previous paper. In retrospect it is maybe not very surprising that the effect of the inner hydrogens was quite small. This could be anticipated, as the ring current was not much affected by the position of the inner hydrogens in most cases.

Having studied a number of aromatic systems, next we turned our interest to some antiaromatic and potentially antiaromatic molecules. In Article IV we studied the ring-current strengths of dehydro[12]annulenes and dehydro[18]annulenes, which are the building blocks of some new carbon allotropes which have been proposed [153, 154, 155, 156]. We found that the unsubstituted dehydro[12]annulene indeed was antiaromatic, but also, that when fused with benzene or cyclobutadiene rings, the antiaromaticity was destroyed in favor of aromaticity of the fused rings. Dehydro[18]annulene was found to be diatropic, but like dehydro[12]annulene, the overall ring current was destroyed upon fusion with benzene or cyclobutadiene. These findings make it unlikely that graphyne or graphdiyne, if ever synthezised, will have any particularly exalted magnetic properties.

In 2001, Wang *et al.* synthesized a new and exciting group of molecules, containing small four membered aluminum rings [115]. The general structure of these molecules is Al_4^-M where M=Li^+, Na^+ or Cu^+. Based on photo-electron spectra and calculations, they concluded that these molecules had significant aromatic character. In Article V, we used the ARCS method to study the ring-current strengths of Al_4^{2-}, and also the group III analogues Ga_4^{2-}, In_4^{2-} and Tl_4^{2-}, and found that they are indeed aromatic. Furthermore, we also proposed a number of new, and neutral, Al_4^{2-} analogues, Si_2B_2, Si_2Al_2 and Si_2Ga_2 all of which should be aromatic. In a forthcoming

paper [7] we have studied a number of Al_4^{2-} and Al_4^{4-} species using the GIMIC method, and found that the diamagnetic part of the ring-current comes from the σ-electrons. In Al_4^{2-} the π-electrons also contribute to the diamagnetic current, making the magnetic response diamagnetic overall. In Al_4^{4-}, however, the π-electrons give rise to a paramagnetic current, effectively canceling the total current. Still, Al_4^{4-} seem to sustain *both* a diatropic and a paratropic current in the same system!

The last class of molecules we studied primarily using the ARCS method, was a group of potentially homoaromatic molecules of the general form $C_nH_{n+1}^x$, with n=4-13 and x=-1,0,+1,+2. These molecules are significantly non-planar since the conjugated ring is interrupted by single bonds. The concept of homoaromaticity has been much debated, and in Article VI we were able to show that of the studied molecules, $C_8H_9^+$ (homotropylium cation), $C_9H_{10}^{2+}$, $C_{10}H_{11}^-$ and $C_{12}H_{13}^+$ can sustain strong ring currents. Article VI also shows some spectacular shortcomings of the NICS method.

The articles discussed so far form a logical whole. Starting from the methodological paper, which included calculations on some simple test systems, in the following papers we apply the method to a variety of systems of much more demanding character, covering most aspects of aromaticity. Although the ARCS method has proven to be very useful and quite reliable, it also became evident that it has a number of limitations. During the work done on porphyrins, it became evident that resolving the ring-current pathways is far from trivial using the ARCS method. Some of the aluminum rings posed their own problems, when the aromatic ring was hindered by counterions, making the ARCS analysis tricky. Finally the work on homoaromatic molecules drew our attention to the problems of non-planar molecules. In these molecules, it is not *a priori* clear how to define an origin for the ARCS points nor the direction which is perpendicular to the ring.

These shortcomings lead to the conclusion that what was needed was an explicit method to calculate the induced current in molecules. Instead of calculating the current indirectly, direct integration of the current through a dividing surface gives a precise measure of the net current in aromatic molecules. Article VII discusses the explicit calculation of magnetically induced currents, presenting the GIMIC method in detail. In the GIMIC paper, we showed how to calculate the current in terms of derivative theory. Using a density matrix formalism, we were able to calculate currents at various levels of theory. The need for correlated wave functions arises when studying difficult species like the Al_4 rings, which require an accurate CCSD wave function to give good results.

The work presented in this thesis is the result of many fruitful collaborations. My own contribution to the methods presented in this thesis has been substantial. When we developed the ARCS method (Articles I and II), I was intimately involved in both developing the ideas for the method as well as in the writing process of the article that resulted. I also single-handedly wrote all the software needed to do the ARCS and PARCS analysis. I was also very much involved in the work, that led to the three papers on porphyrins, magnesium porphyrins and dehydroannulenes (Articles II-IV). My input involved ideas on how to resolve the structure of the current, doing the actual calculations and also partially writing the articles. My contribution to the papers on Al_4^{2-} and homoaromatic molecules (Articles V and VI) is more technical, doing part of the calculations and all of the ARCS calculations, and I do not want to claim much credit for the original ideas presented in the papers. Finally, already while working on the ARCS method, I realized the need for a method capable of explicitly calculating the induced current density and integrating the current, on order to obtain a better aromaticity index. The ideas of how this could be done, were born in a collaboration with Dage Sundholm and Jürgen Gauss. During my first visit to Mainz I derived the necessary theory needed for a computer implementation. Subsequently I implemented the theory in the computer program GIMIC, which has been used for all explicit current calculations presented in this thesis. The paper on the GIMIC method (Article VII), is to a large extent written by myself.

References

[1] J. Jusélius and D. Sundholm, *Ab initio determination of the induced ring current in aromatic molecules*, Phys. Chem. Chem. Phys., **1**, 3429 (1999).

[2] J. Jusélius and D. Sundholm, *The aromatic pathways of porphins, chlorins and bacteriochlorins*, Phys. Chem. Chem. Phys., **2**, 2145 (2000).

[3] J. Jusélius and D. Sundholm, *The aromatic character of magnesium porphyrins*, J. Org. Chem., **65**, 5233 (2000).

[4] J. Jusélius and D. Sundholm, *The aromaticity and antiaromaticity of dehydroannulenes*, Phys. Chem. Chem. Phys., **3**, 2433 (2001).

[5] J. Jusélius, M. Straka, and D. Sundholm, *Magnetic Shielding Calculations on Al_4^{2-} and Analogues*, J. Phys. Chem. A, **105**, 9939 (2001).

[6] J. Jusélius, M. Patzschke, and D. Sundholm, *Calculation of Ring-Current Susceptibilites for Potentially Homoaromatic Hydrocarbons*, J. Mol. Struct. (Theochem), **633**, 123 (2003).

[7] J. Jusélius, D. Sundholm, and J. Gauss, *Calculation of Current Densities using Gauge-Including Atomic Orbitals*, J. Chem. Phys., **121**, 3952 (2004).

[8] R. J. F. Berger, M. A. Schmidt, J. Jusélius, D. Sundholm, P. Sirsch, and H. Schmidbaur, *Tetraberyllium-η^4-oxo-hexa(arylcarboxylates)*, Z. Naturforsch. b, **56**, 979 (2001).

[9] E. M. S. Maçôas, L. Khriachtchev, M. Petterson, J. Jusélius, R. Fausto, and M. Räsänen, *Reactive vibrational excitation spectroscopy of formic acid in solid argon: Quantum yield for infrared induced trans→cis isomerization and solid state effects on the vibrational spectrum*, J. Chem. Phys., **119**, 11765 (2004).

[10] M. Johansson and J. Jusélius, *Arsole aromaticity revisited*, Lett. Org. Chem. (2004), accepted.

[11] L. Khriachtchev, J. Jusélius, A. Lignell, M. Räsänen, and E. Savchenko, *Infrared absorption spectrum of matrix-isolated noble-gas hydride molecules: Fingerprints of specific interactions and hindered rotation*, J. Chem. Phys. (2004), accepted.

[12] D. Sundholm, M. Johansson, and J. Jusélius, *Sphere currents of Buckminsterfullerene*, Angew. Chem. Int. Ed. (2004), accepted.

[13] Y. C. Lin, J. Jusélius, D. Sundholm, and J. Gauss, *Calculation of Current Densities in Al_4^{2-}*, Angew. Chem. Int. Ed. (2004), to be published.

[14] U. Fleischer, W. Kutzelnigg, P. Lazzeretti, and V. Mühlenkamp, J. Am. Chem. Soc., **116**, 5298 (1994).

[15] J. A. Elvidge and L. M. Jackman, J. Chem. Soc., p. 859 (1961).

[16] R. J. Abraham, R. C. Sheppard, W. A. Thomas, and S. Turner, Chem. Comm., **43** (1965).

[17] P. von Ragué Schleyer, C. Maerker, A. Dransfeld, H. Jiao, and N. J. R. van Eikema Hommes, J. Am. Chem. Soc., **118**, 6317 (1996).

[18] G. Subramanian, P. von Ragué Schleyer, and H. Jiao, Angew. Chem. Int. Ed., **35**, 2638 (1996).

[19] M. Bühl, Chem. Eur. J., **4**, 734 (1998).

[20] A. Julg and P. François, Theoret. Chim. Acta, **8**, 249 (1967).

[21] C. W. Bird, Tetrahedron, **41**, 1409 (1985).

[22] K. Jug and A. Köster, J. Phys. Org. Chem., **4**, 163 (1991).

[23] V. I. Minkin, M. N. Glukhovtsev, and B. Y. Simkin, *Aromaticity and Antiaromaticity - Electronic and Structural Aspects* (Wiley, New York, 1994).

[24] P. von Ragué Schleyer, P. K. Freeman, H. Jiao, and B. Goldfuss, Angew. Chem. Int. Ed., **34**, 337 (1995).

[25] H. Jiao, P. von Ragué Schleyer, and M. N. Glukhovtsev, J. Phys. Chem., **110**, 12299 (1996).

[26] P. von Ragué Schleyer and H. Jiao, Pure Appl. Chem., **28**, 209 (1996).

[27] I. Černušák, P. W. Fowler, and E. Steiner, Mol. Phys., **91**, 401 (1997).

[28] R. Zanasi and P. Lazzeretti, Mol. Phys., **92**, 609 (1997).

[29] M. K. Cyrañski, T. M. Krygowski, M. Wisiorowski, N. J. R. van Eikema Hommes, and P. von Ragué Schleyer, Angew. Chem. Int. Ed., **37**, 177 (1998).

[30] M. Born and J. R. Oppenheimer, Ann. Physik, **84**, 458 (1927).

[31] S. Gasiorowicz, *Quantum Physics* (Wiley, 1996).

[32] R. McWeeny, *Methods of Molecular Quantum Mechanics* (Academic Press, 1992).

[33] P. O. Lövdin, Rev. Mod. Phys., **34**, 80 (1962).

[34] R. J. Bartlett and G. D. Purvis, Int. J. Quantum Chem., **14**, 561 (1978).

[35] J. A. Pople, J. S. Binkley, and R. Seeger, Int. J. Quantum Chem., **S10**, 1 (1976).

[36] J. Olsen, O. Christiansen, H. Koch, and P. Jørgensen, J. Chem. Phys., **105**, 5082 (1996).

[37] T. Helgaker, P. Jørgensen, and J. Olsen, *Molecular Electronic-Structure Theory* (Wiley, West Sussex, England, 2000).

[38] T. D. Crawford and H. F. Schaefer, *An Introduction to Coupled Cluster Theory for Computational Chemists* (2000).

[39] J. L. Whitten, J. Chem. Phys., **58**, 4496 (1973).

[40] M. Feyereisen, G. Fitzgerald, and A. Komornicki, Chem. Phys. Lett., **208**, 359 (1993).

[41] M. C. Strain, G. E. Scuseria, and M. J. Frisch, Science, **271**, 51 (1996).

[42] C. A. White, B. G. Johnson, P. M. W. Gill, and M. Head-Gordon, Chem. Phys. Lett., **253**, 268 (1996).

[43] M. Schütz, G. Hetzer, and H. J. Werner, J. Chem. Phys., **111**, 5691 (1999).

[44] M. Schütz and H. J. Werner, J. Chem. Phys., **114**, 661 (2001).

[45] P. Hohenberg and W. Kohn, Phys. Rev. B, **136**, 864 (1964).

[46] W. Kohn and L. J. Sham, Phys. Rev., **140**, 1133 (1965).

[47] A. D. Becke, J. Chem. Phys., **98**, 5648 (1993).

[48] C. Lee, W. Yang, and R. G. Parr, Phys. Rev. B, **37**, 785 (1988).

[49] S. Hirata, S. Ivanov, I. Grabowski, R. J. Bartlett, K. Burke, and J. D. Talman, J. Chem. Phys., **115**, 1635 (2001).

[50] A. Görling, Phys. Rev. Lett., **83**, 5459 (1999).

[51] K. Eichkorn, O. Treutler, H. Öhm, M. Häser, and R. Ahlrichs, Chem. Phys. Lett., **240**, 283 (1995).

[52] B. I. Dunlap, J. W. D. Connolly, and J. R. Sabin, J. Chem. Phys., **71**, 3396 (1979).

[53] O. Vahtras, J. Almlöf, and M. V. Feyereisen, Chem. Phys. Lett., **213**(5-6), 514 (1993).

[54] D. E. Bernholdt and R. J. Harrison, Chem. Phys. Lett., **250**(5-6), 477 (1996).

[55] F. Weigend, M. Häser, H. Patzelt, and R. Ahlrichs, Chem. Phys. Lett., **294**(1-3), 143 (1998).

[56] F. Weigend, Phys. Chem. Chem. Phys., **4**, 4285 (2002).

[57] K. Ruud, *Magnetic properties of closed-shell molecules*, Ph.D. thesis, Department of Chemistry, University of Oslo (1998).

[58] J. Gerratt and I. M. Mills, J. Chem. Phys., **49**, 1719 (1968).

[59] P. Szalay, M. Nooijen, and R. J. Bartlett, J. Chem. Phys., **103**, 281 (1994).

[60] A. Szabo and N. S. Ostlund, *Modern Quantum Chemistry* (Dover Publications, 1996).

[61] J. Gauss, *Ab initio Berechnung chemischer NMR-Verschiebungen unter Berücksichtigung der Elektronenkorrelation*, Habilitation thesis (University of Karlsruhe, 1993).

[62] J. Gauss, J. Chem. Phys., **99**, 3629 (1993).

[63] R. McWeeny, Rev. Mod. Phys., **32**, 335 (1960).

[64] R. McWeeny, Phys. Rev., **116**, 1028 (1962).

[65] R. M. Stevens, R. M. Pitzer, and W. N. Lipscomb, J. Chem. Phys., **38**, 550 (1963).

[66] N. C. Handy and H. F. Schaefer, J. Chem. Phys., **81**, 5031 (1984).

[67] W. H. Flygare, Chem. Rev., **74**(6), 653 (1974).

[68] D. W. Davies, *The Theory of the Electric and Magnetic Properties of Molecules* (John Wiley & Sons, London, 1967).

[69] P. Lazzeretti, Prog. Nucl. Magn. Res. Spectr., **36**, 1 (2000).

[70] S. T. Epstein, J. Chem. Phys., **58**, 1592 (1973).

[71] C. V. Lanczos, *The Variational Principles of Mechanics* (University of Toronto Press, 1970).

[72] S. T. Epstein, J. Chem. Phys., **42**, 2897 (1964).

[73] J. Gauss and J. F. Stanton, J. Chem. Phys., **103**, 3561 (1995).

[74] A. E. Hansen and T. D. Bouman, in J. A. Tossell (ed.), *Nuclear Magnetic Shieldings and Molecular Structure*, vol. 386, p. 117 (Kluwer Academic Publishers, NATO ASI Series C, 1993).

[75] W. Kutzelnigg, C. van Wüllen, U. Fleischer, R. Franke, and T. van Mourik, *The IGLO method. Recent developments*, in J. A. Tossell (ed.), *Nuclear Magnetic Shieldings and Molecular Structure*, pp. 141–161 (Kluwer Academic Publishers, NATO ASI Series C, 1993).

[76] T. D. Bouman and A. E. Hansen, Chem. Phys. Lett., **175**, 292 (1990).

[77] C. van Wüllen and W. Kutzelnigg, Chem. Phys. Lett., **205**, 653 (1993).

[78] F. London, J. Phys. Radium, **8**, 397 (1937).

[79] J. Gauss, K. Ruud, and T. Helgaker, J. Chem. Phys., **105**, 2804 (1996).

[80] J. A. Pople, Proc. R. Soc., London, **239**, 541 (1957).

[81] J. A. Pople, Proc. R. Soc., London, **239**, 550 (1957).

[82] H. Hameka, Mol. Phys., **1**, 203 (1958).

[83] R. Ditchfield, Mol. Phys., **27**, 789 (1974).

[84] D. B. Chesnut and C. K. Foley, Chem. Phys. Lett., **118**, 316 (1985).

[85] D. B. Chesnut and K. D. Moore, J. Comp. Chem., **10**, 648 (1985).

[86] K. Wolinski, J. F. Hinton, and P. Pulay, J. Am. Chem. Soc., **112**, 8251 (1990).

[87] P. Pulay, J. F. Hinton, and K. Wolinski, in J. A. Tossell (ed.), *Nuclear Magnetic Shieldings and Molecular Structure*, vol. 386, p. 243 (Kluwer Academic Publishers, NATO ASI Series C, 1993).

[88] P. Pulay, in D. R. Yarkony (ed.), *Modern Electronic Structure Theory*, vol. 2, p. 1191 (World Scientific, Singapore, 1995).

[89] R. Ahlrichs, M. Bär, M. Häser, H. Horn, and C. Kölmel, *Electronic Structure Calculations on Workstation Computers: The Program System TURBOMOLE*, Chem. Phys. Lett., **162**, 165 (1989).

[90] J. F. Stanton, J. Gauss, J. D. Watts, W. J. Lauderdale, and R. J. Bartlett, Intern. J. Quantum Chem. Symp., **26**, 879 (1992), ACESII, an ab initio program system, authored by J. F. Stanton, J. Gauss, J. D. Watts, W. J. Lauderdale and R. J. Bartlett, which includes modified versions of the MOLECULE Gaussian integral program of J. Almlöf and P. R. Taylor, the ABACUS integral derivative program written by T. Helgaker, H. J. Aa. Jensen, P. Jørgensen and P. R. Taylor, and the PROPS property integral code of P.R. Taylor.

[91] T. Helgaker, H. J. Aa. Jensen, P. Jørgensen, J. Olsen, K. Ruud, H. Ågren, A. A. Auer, K. L. Bak, V. Bakken, O. Christiansen, S. Coriani, P. Dahle, E. K. Dalskov, T. Enevoldsen, B. Fernandez, C. Hättig, K. Hald, A. Halkier, H. Heiberg, H. Hettema, D. Jonsson, S. Kirpekar, R. Kobayashi, H. Koch, K. V. Mikkelsen, P. Norman, M. J. Packer, T. B. Pedersen, T. A. Ruden, A. Sanchez, T. Saue, S. P. A. Sauer, B. Schimmelpfennig, K. O. Sylvester-Hvid, P. R. Taylor, and O. Vahtras, *Dalton, a molecular electronic structure program, Release 1.2* (2001).

[92] K. Ruud, T. Helgaker, R. Kobayashi, P. Jørgensen, K. L. Bak, and H. J. Aa. Jensen, J. Chem. Phys., **100**, 8178 (1994).

[93] J. Gauss, Chem. Phys. Lett., **191**, 614 (1992).

[94] M. Häser, R. Ahlrichs, H. P. Baron, P. Weis, and H. Horn, Theoret. Chim. Acta, **83**, 551 (1992).

[95] J. R. Cheeseman, G. W. Trucks, T. A. Keith, and M. J. Frisch, J. Chem. Phys., **104**, 5497 (1996).

[96] A. M. Lee, N. C. Handy, and S. M. Colwell, J. Chem. Phys., **103**, 10095 (1995).

[97] T. Helgaker, M. Jaszuński, and K. Ruud, Chem. Rev., **99**, 293 (1999).

[98] J. Gauss, Chem. Phys. Lett., **229**, 198 (1994).

[99] J. Gauss and J. F. Stanton, J. Chem. Phys., **102**, 251 (1995).

[100] G. Schreckenbach and T. Ziegler, J. Phys. Chem., **99**, 606 (1995).

[101] J. Gauss and J. F. Stanton, J. Chem. Phys., **104**, 2574 (1996).

[102] G. Rauhut, S. Puyear, K. Wolinski, and P. Pulay, J. Phys. Chem., **100**, 6310 (1996).

[103] J. Gauss and J. F. Stanton, Phys. Chem. Chem. Phys., **2**, 2047 (2000).

[104] J. Gauss, J. Chem. Phys., **116**, 4773 (2002).

[105] M. Kállay and J. Gauss, J. Chem. Phys., **120**, 6841 (2004).

[106] E. Hückel, Z. Physik, **70**, 204 (1931).

[107] E. Hückel, Z. Physik, **72**, 310 (1931).

[108] K. Wüthrich, G. Wider, G. Wagner, and W. Braun, J. Mol. Biol., **155**, 311 (1982).

[109] E. Steiner and P. Fowler, J. Phys. Chem. A, **105**, 9553 (2001).

[110] E. Steiner and P. Fowler, Chem. Comm., p. 2220 (2001).

[111] M. Faraday, Phil. Trans. Roy. Soc., p. 440 (1825).

[112] J. Jusélius, *Ab Initio-beräkning av inducerade ringströmmar i aromatiska molekyler*, Master's thesis, Department of Chemistry, University of Helsinki (2000).

[113] H. C. Ohanian, *Physics* (WW Norton Company, 1989), 2 edn.

[114] J. A. Pople and K. G. Untch, J. Am. Chem. Soc., **88**, 4811 (1966).

[115] X. Li, A. E. Kuznetsov, H.-F. Zhang, A. I. Boldyrev, and L.-S. Wang, Science, **291**, 859 (2001).

[116] S. Winstein, J. Am. Chem. Soc., **81**, 6524 (1959).

[117] R. F. Childs, J. Am. Chem. Soc., **17**, 347 (1984).

[118] R. V. Williams, Chem. Rev., **101**, 1185 (2001).

[119] A. Hirsch, Z. Chen, and H. Jiao, Angew. Chem. Int. Ed., **39**, 3915 (2000).

[120] Z. Chen, H. Jiao, A. Hirsch, and W. Thiel, J. Mol. Model., **7**, 161 (2001).

[121] G. Van Lier, P. W. Fowler, F. De Proft, and P. Geerlings, J. Phys. Chem. A, **106**, 5128 (2002).

[122] M. Bühl and A. Hirsch, Chem. Rev., **101**, 1153 (2001).

[123] A. Hirsch, Z. Chen, and H. Jiao, Angew. Chem. Int. Ed., **40**, 2834 (2001).

[124] A. Hirsch, Z. Chen, and H. Jiao, in *From Synthesis to Optoelectronic Applications*, pp. 121–135 (Kluwer Academic Publishers, Dordrecht, 2002).

[125] Z. Chen, T. Heine, D. Sundholm, and P. von Ragué Schleyer, in M. Kaupp, M. Bühl, and V. Malkin (eds.), *Quantum Chemical Calculation of Magnetic Resonance Properties*, pp. 395–407 (Wiley-VCH, Weinheim, Germany, 2004).

[126] M. P. Johansson, D. Sundholm, and J. Vaara, Angew. Chem. Int. Ed., **43**, 2678 (2004).

[127] J. Lounila, M. Ala-Korpela, J. Jokisaari, M. J. Savolainen, and Y. A. Kesäniemi, Phys. Rev. Lett., **72**, 4049 (1994).

[128] E. Heilbronner, Tetrahedron Lett., p. 1923 (1964).

[129] C. Castro, C. M. Isborn, W. L. Karney, M. Mauksch, P. von Ragué Schleyer, and H. Jiao, Org. Lett., **4**, 3431 (2002).

[130] P. Lazzeretti, Phys. Chem. Chem. Phys., **6**, 217 (2004).

[131] S. Klod and E. Kleinpeter, J. Chem. Soc., Perkin Trans. 2, pp. 1893–1998 (2001).

[132] S. Klod and E. Kleinpeter, J. Chem. Soc., Perkin Trans. 2, pp. 1506–1509 (2002).

[133] G. Merino, T. Heine, and G. Seifert, Chem. Eur. J., **10**, 4367 (2004).

[134] G. Arfken, *Mathematical Methods for Physicists* (Academic Press, Orlando, 1985).

[135] K. Lonsdale, Proc. R. Soc., London A, **159**, 149 (1937).

[136] L. Pauling, J. Chem. Phys., **4**, 637 (1936).

[137] J. A. Pople, J. Chem. Phys., **24**, 1111 (1956).

[138] J. Gauss and J. F. Stanton, Adv. Chem. Phys., **123**, 355 (2002).

[139] T. A. Keith and R. F. W. Bader, Chem. Phys. Lett., **210**, 223 (1993).

[140] R. F. W. Bader and T. A. Keith, J. Chem. Phys., **99**, 3683 (1993).

[141] P. Lazzeretti, in P. von Ragué Schleyer, N. L. Allinger, T. Clark, J. Gasteiger, P. A. Kollman, H. F. Schaefer III, and P. R. Schreiner (eds.), *Encyclopedia of Computational Chemistry*, vol. 3, p. 1659 (Wiley, 1998).

[142] D. F. Heller and J. O. Hirshfelder, J. Chem. Phys., **66**, 1929 (1977).

[143] P. Lazzeretti, M. Malagoli, and R. Zanasi, Chem. Phys. Lett., **220**, 299 (1994).

[144] S. Coriani, P. Lazzeretti, M. Malagoli, and R. Zanasi, Theor. Chim. Acta, **89**, 181 (1994).

[145] R. Zanasi, P. Lazzeretti, M. Malagoli, and F. Piccinini, J. Chem. Phys., **102**, 7150 (1995).

[146] R. Zanasi, J. Chem. Phys., **105**, 1460 (1996).

[147] P. W. Fowler, R. Zanasi, B. Cadioli, and E. Steiner, Chem. Phys. Lett., **251**, 132 (1996).

[148] P. W. Fowler, E. Steiner, B. Cadioli, and R. Zanasi, J. Phys. Chem. A, **102**, 7297 (1998).

[149] T. K. Rebane, Sov. Phys. JETP, **11**, 694 (1960).

[150] F. R. Salsbury Jr and R. A. Harris, J. Chem. Phys., **104**, 5497 (1996).

[151] T. A. Keith, Chem. Phys, **213**, 123 (1996).

[152] M. Abramowitz and I. A. Stegun (Eds.), in *Handbook of Mathematical Functions* (Dover, 1965).

[153] M. M. Haley, S. C. Brand, and J. J. Pak, Angew. Chem. Int. Ed., **36**, 836 (1997).

[154] C. Eickmeier, H. Junga, A. J. Matzger, F. Scherhag, M. Shim, and K. P. Vollhardt, Angew. Chem. Int. Ed., **36**, 2103 (1997).

[155] W. B. Wan, S. C. Brand, J. J. Pak, and M. M. Haley, Chem. Eur. J., **6**, 2044 (2000).

[156] F. Diederich and Y. Rubin, Angew. Chem. Int. Ed., **104**, 1123 (1992).

Article I

J. Jusélius and D. Sundholm, *Ab initio determination of the induced ring current in aromatic molecules*, Phys. Chem. Chem. Phys., **1**, 3429 (1999).

Article II

J. Jusélius and D. Sundholm, *The aromatic pathways of porphins, chlorins and bacteriochlorins*, Phys. Chem. Chem. Phys., **2**, 2145 (2000).

Article III

J. Jusélius and D. Sundholm, *The aromatic character of magnesium porphyrins*, J. Org. Chem., **65**, 5233 (2000).

Article IV

J. Jusélius and D. Sundholm, *The aromaticity and antiaromaticity of dehydroannulenes*, Phys. Chem. Chem. Phys., **3**, 2433 (2001).

Article V

J. Jusélius, M. Straka, and D. Sundholm, *Magnetic Shielding Calculations on* Al_4^{2-} *and Analogues*, J. Phys. Chem. A, **105**, 9939 (2001).

Article VI

J. Jusélius, M. Patzschke, and D. Sundholm, *Calculation of Ring-Current Susceptibilites for Potentially Homoaromatic Hydrocarbons*, J. Mol. Struct. (Theochem), **633**, 123 (2003).

Article VII

J. Jusélius, D. Sundholm, and J. Gauss, *Calculation of Current Densities using Gauge-Including Atomic Orbitals*, J. Chem. Phys., **121**, 3952 (2004).